Tissue-resident PSGL1^{lo}CD4^{+} T cells promote B cell differentiation and chronic graft-versus-host disease–associated autoimmunity

Xiaohui Kong,[1,2] Deye Zeng,[1,2,3] Xiwei Wu,[4] Bixin Wang,[1,2,5] Shijie Yang,[1,2,6] Qingxiao Song,[1,2,5] Yongping Zhu,[1,2] Martha Salas,[1,2] Hanjun Qin,[4] Ubaydah Nasri,[1,2] Karen M. Haas,[7] Arthur D. Riggs,[1] Ryotaro Nakamura,[2] Paul J. Martin,[8] Aimin Huang,[3] and Defu Zeng[1,2]

[1]Diabetes and Metabolism Research Institute, the Beckman Research Institute of City of Hope, Duarte, California, USA. [2]Hematologic Malignancies and Stem Cell Transplantation Institute, City of Hope National Medical Center, Duarte, California, USA. [3]Department of Pathology at School of Basic Medical Sciences, Institute of Oncology and Diagnostic Pathology Center, Fujian Medical University, Fuzhou, China. [4]Department of Integrative Genomics Core, The Beckman Research Institute of City of Hope, Duarte, California, USA. [5]Fujian Medical University Center of Translational Hematology, Fujian Institute of Hematology, Fujian Medical University Union Hospital, Fuzhou, China. [6]Department of Hematology, Xinqiao Hospital of Army Medical University, Chongqing, China. [7]Department of Microbiology and Immunology, Wake Forest School of Medicine, Winston-Salem, North Carolina, USA. [8]Fred Hutchinson Cancer Research Center, Seattle, Washington, USA.

CD4^{+} T cell interactions with B cells play a critical role in the pathogenesis of systemic autoimmune diseases such as systemic lupus and chronic graft-versus-host disease (cGVHD). Extrafollicular CD44^{hi}CD62L^{lo}PSGL1^{lo}CD4^{+} T cells (PSGL1^{lo}CD4^{+} T cells) are associated with the pathogenesis of lupus and cGVHD, but their causal role has not been established. With murine and humanized MHC$^{-/-}$HLA-A2^{+}DR4^{+} murine models of cGVHD, we showed that murine and human PSGL1^{lo}CD4^{+} T cells from GVHD target tissues have features of B cell helpers with upregulated expression of programmed cell death protein 1 (PD1) and inducible T cell costimulator (ICOS) and production of IL-21. They reside in nonlymphoid tissues without circulating in the blood and have features of tissue-resident memory T cells with upregulated expression of CD69. Murine PSGL1^{lo}CD4^{+} T cells from GVHD target tissues augmented B cell differentiation into plasma cells and production of autoantibodies via their PD1 interaction with PD-L2 on B cells. Human PSGL1^{lo}CD4^{+} T cells were apposed with memory B cells in the liver tissues of humanized mice and cGVHD patients. Human PSGL1^{lo}CD4^{+} T cells from humanized GVHD target tissues also augmented autologous memory B cell differentiation into plasma cells and antibody production in a PD1/PD-L2–dependent manner. Further preclinical studies targeting tissue-resident T cells to treat antibody-mediated features of autoimmune diseases are warranted.

Introduction

Systemic autoimmune diseases such as systemic lupus erythematosus (SLE) and chronic graft-versus-host disease (cGVHD) are mediated by abnormal CD4^{+} T cell interaction with B cells and autoantibody deposition in target tissues such as the kidney and skin (1–4). The exacerbated autoimmunity in SLE is associated with enlarged germinal centers (GC), in which T follicular helper (Tfh) cells' interactions with GC B cells lead to the production of long-lived plasma cells and high-affinity IgG antibodies with somatic hypermutation (5). Tfh cells express high levels of PD1 that interact with PD-L2 on GC B cells to augment antibody production (6), although PD1$^{-/-}$ mice still develop autoimmune syndromes with high concentrations of autoantibodies in the serum (7).

P selectin glycoprotein ligand 1 (PSGL1, also known as CD162) is widely expressed in almost all T cells in the blood and binds to E selectin and P selectin after appropriate glycosylation and tyrosine sulfation, which regulates migration of immune cells into tissues (8). A subset of activated CD4^{+} T cells in the spleen of SLE mice downregulates expression of PSGL1, and they become CD44^{hi}CD62L^{-}PSGL1^{lo}CD4^{+} T cells (PSGL1^{lo}CD4^{+} T cells) (9). PSGL1^{lo}CD4^{+} T cells localize at the extrafollicular sites of systemic lupus mice, and they express high levels of CXCR4, ICOS, and CD40L without expression of CXCR5 (1). Unlike GC CXCR5^{+}Tfh CD4^{+} T cell development, CXCR4^{+}PSGL1^{lo}CD4^{+} T cells develop outside GCs in an ICOS-dependent manner (9). PSGL1^{lo}CD4^{+} T cells from the spleen of SLE mice augment autoantibody production through IL-21 and CD40L in vitro, and they have been designated as extrafollicular B cell helpers (1, 9). However, it remains unclear whether PSGL1^{lo}CD4^{+} T cells interact with B cells in nonlymphoid tissues of autoimmune mice. In addition, PSGL1^{lo}CD4^{+} T cells in humans have not yet been reported.

cGVHD often occurs as a sequela of acute GVHD (aGVHD) (10). GVHD is a severe side effect of allogeneic hematopoietic cell transplantation (allo-HCT), in which alloreactive T cells attack target organs such as the gut, liver, lung, and skin (11). aGVHD is an acute inflammatory response mainly mediated by infiltrating alloreactive T cells, whereas cGVHD is mediated by autoreactive CD4^{+} T cells derived from T cells in the graft (12–14) and from failure of negative selection in the thymus (15, 16), by aberrant B cell signaling (17), and by abnormal CD4^{+} T and B

Authorship note: XK and Deye Zeng contributed equally to this work.
Conflict of interest: The authors have declared that no conflict of interest exists.

Submitted: December 4, 2019; **Accepted:** September 9, 2020; **Published:** January 4, 2021.
Reference information: *J Clin Invest*. 2021;131(1):e135468.
https://doi.org/10.1172/JCI135468.

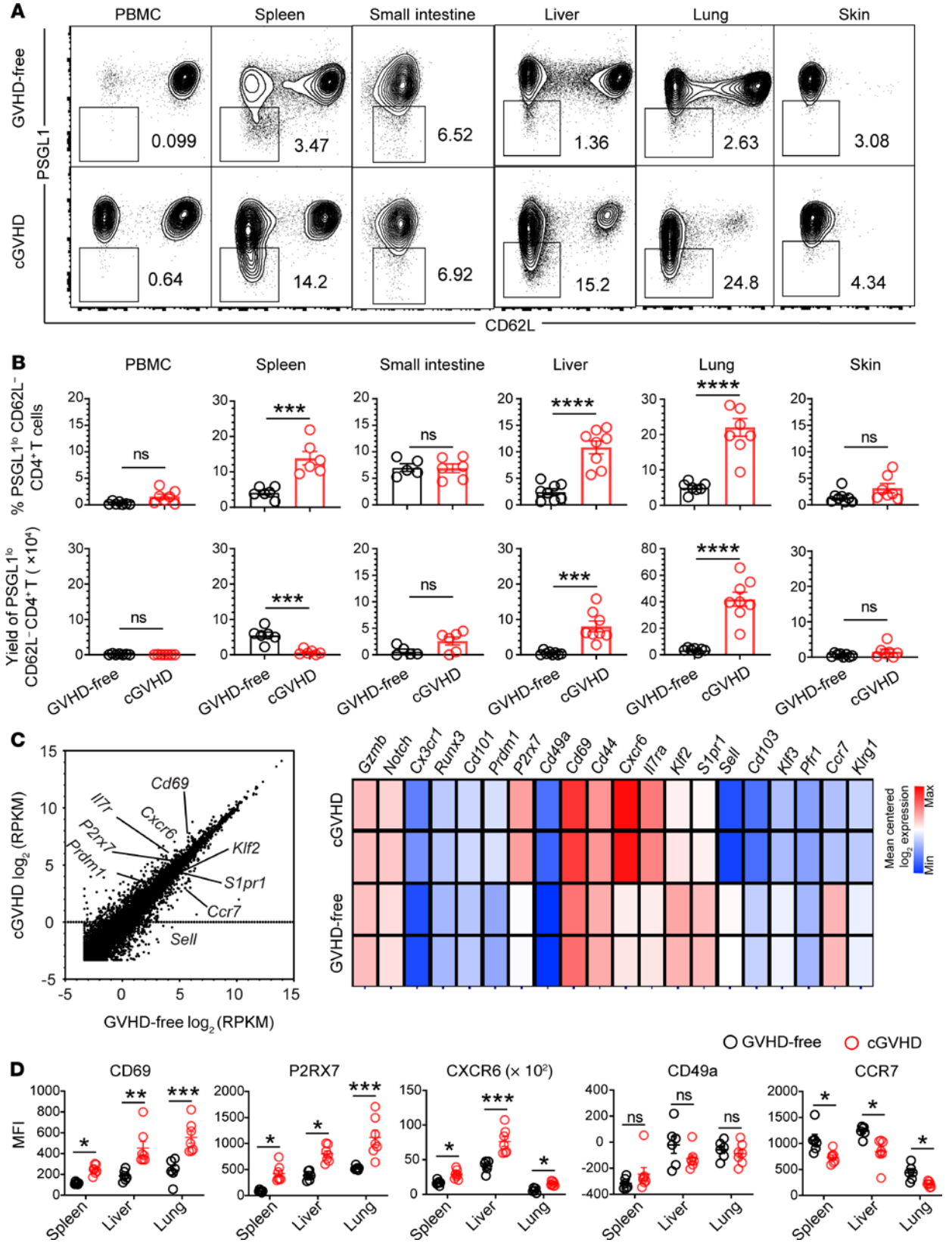

J Clin Invest. 2021;131(1):e135468 https://doi.org/10.1172/JCI135468

Figure 1. PSGL1^{lo}CD4$^+$ T cells reside in the liver and lung. Lethally irradiated BACL/c (H-2^d) mice received TCD-BM plus splenocytes (cGVHD group) or TCD-BM alone (GVHD-free group) from C57BL/6 (H-2^b) donors. (**A**) At 60 days after HCT, mononuclear cells from the PBMCs, spleen, small intestine, liver, lung, and skin were stained with anti–H-2Kb, TCRβ, CD4, CD62L, and PSGL1. (**B**) Mean ± SEM of the percentage among donor-type CD4$^+$ T cells and yield of donor-type H-2Kb$^+$PSGL1^{lo}CD62L$^-$CD4$^+$TCRβ$^+$ cells are shown. *N* = 6–8, combined from 3 replicate experiments. (**C**) Scatter plot comparing PSGL-1^{lo}CD62L$^-$CD4$^+$ T cells from GVHD-free and cGVHD recipients. The heatmap shows the core genes associated with tissue residency. Duplicated samples are pooled from 6–10 GVHD-free recipients or cGVHD recipients, respectively. (**D**) Surface expression of CD69, P2RX7, CXCR6, CD49a, and CCR7 of the PSGL1^{lo}CD62L$^-$CD4$^+$ T cells was measured. Mean ± SEM of MFI is shown, *N* = 6–8, combined from 3 independent experiments. *P* values were calculated by unpaired 2-tailed Student's *t* tests (**B**) or by 1-way ANOVA multiple-comparisons test (**D**). $^*P < 0.05$; $^{**}P < 0.01$; $^{***}P < 0.001$; $^{****}P < 0.0001$.

interactions due to lack of donor-derived Treg cells (2, 18). CD4$^+$ T cell interaction with B cells augments cGVHD via clonal expansion of pathogenic CD4$^+$ T cells and autoantibody production (4).

Others have reported that cGVHD pathogenesis was associated with enlarged GCs and that BCL6 deficiency in donor B cells prevented cGVHD (19). We recently reported that cGVHD causes destruction of lymphoid follicles and absence of GCs in the lymphoid tissues (20). cGVHD pathogenesis did not require donor B cell expression of BCL6 or GC formation, and development of the disease was associated with the expansion of extrafollicular CXCR5$^-$BCL6$^+$PSGL1^{lo}CD4$^+$ T cells in GVHD target tissues (20). Our previous study left several important questions unanswered. How do PSGL1^{lo}CD4$^+$ T cells in the GVHD target tissues interact with B cells? Do PSGL1^{lo}CD4$^+$ T cells circulate in the blood? To what extent do murine and human PSGL1^{lo}CD4$^+$ T cells from GVHD target tissues have a similar phenotype and function?

Tissue-resident memory T cells (Trm cells) are CD44^{hi}CD62L$^-$ with high expression of CD69, CD103, CD49a, CD101, and P2RX7, but low expression of KLF2/3, S1PR1, and CCR7 (21). The low expression of S1PR1, CCR7, and CD62L restricts their egress from tissues into the circulation and ensures their residency in tissues (21). In addition, Blimp-1, Hobit, Runx3, and Notch are transcription factors that regulate Trm cell development and maintenance (21). Trm cells in healthy tissues serve as a front line of defense against pathogens in the gut, skin, and lung (22). Trm cells also play an essential role in inducing local humoral responses by recruiting B cells during infection (23). Previous studies have not established whether Trm cells interact directly with B cells.

Autoimmune-like cGVHD can emerge after aGVHD or after HCT without preceding aGVHD (16, 18, 24). In the current studies, we used a murine model of cGVHD that emerged after aGVHD (16) and a newly established humanized MHC$^{-/-}$HLA-A2$^+$DR4$^+$ mouse model of cGVHD to show that tissue-resident murine and human PSGL1^{lo}CD4$^+$ T cells augmented memory B cell differentiation into plasma cells and production of autoantibodies in a PD1– and PD-L2–dependent manner.

Results

Expansion of PSGL^{lo}CD4$^+$ T cells is observed in the liver and lungs of recipients with overt cGVHD, but not in those with mild cGVHD. We induced overt cGVHD and mild cGVHD by injecting spleen cells (1.0 or 0.1 × 10^6) and T cell–depleted bone marrow cells (TCD-BM, 2.5 × 10^6) from MHC-mismatched C57BL/6 donors into lethal total body irradiation–conditioned (TBI-conditioned) BALB/c recipients, as previously described (16, 20). Recipients given TCD-BM alone were used as GVHD-free controls. Recipients given 1 × 10^6 spleen cells developed overt cGVHD with body weight loss, hair loss, and mortality, and approximately 37% survived for more than 60 days. Recipients given 0.1 × 10^6 donor spleen cells developed mild cGVHD with some weight loss, but no clear hair loss or mortality, and all survived for more than 60 days (Supplemental Figure 1A; supplemental material available online with this article; https://doi.org/10.1172/JCI135468DS1). Although the numbers of PSGL1^{lo}CD4$^+$ T cells were not increased in the liver, they were significantly increased in the lung at 60 days after HCT in recipients with mild cGVHD compared with GVHD-free recipients, and they were greatly expanded in the liver and lung of recipients with overt cGVHD (Supplemental Figure 1B). As indicated by the presence of Tfh cells and GC B cells, splenic GCs persisted in recipients with mild cGVHD, but could not be detected in recipients with overt cGVHD (Supplemental Figure 1C).

PSGL1^{lo}CD4$^+$ T cells are absent in the peripheral blood and skin, but expanded in the liver and lungs of overt cGVHD recipients. At 60 days after HCT, recipients with overt cGVHD had moderate cellular infiltration and clear collagen deposition in the liver, lung, skin, and salivary gland, as well as IgG antibody deposition in the liver, lung, skin, and thymus tissues (Supplemental Figure 2, A–C). The percentage and yield of PSGL1^{lo}CD4$^+$ T cells were much higher in the liver and lungs of cGVHD recipients compared with GVHD-free recipients. PBMCs and skin mononuclear cells from GVHD-free or cGVHD recipients contained few PSGL1^{lo}CD4$^+$ T cells, with no differences between the 2 groups. The percentage and yield of PSGL1^{lo}CD4$^+$ T cells among mononuclear cells from intestinal tissues were low in GVHD-free and cGVHD recipients, with no difference between the 2 groups (Figure 1, A and B). At the onset of cGVHD, 30 days after HCT, PSGL^{lo}CD4$^+$ T cells were not detectable in the blood or skin, whereas the percentage and yield of PSGL1^{lo}CD4$^+$ T cells were much higher in the liver and lung of cGVHD recipients compared with GVHD-free recipients (Supplemental Figure 3, A and B). Although donor-derived B cells were present in the liver of GVHD-free and cGVHD recipients on days 30 and 60 after HCT, they were nearly absent in the skin (Supplemental Figure 3C).

PSGL^{lo}CD4$^+$ T cells in the GVHD target tissues are Trm cells. At day 30 after HCT, nearly all PSGL1^{lo}CD4$^+$ T cells in the liver and lungs were derived from the donor CD4$^+$ T cells in the graft. By day 60, PSGL1^{lo}CD4$^+$ cells derived from the marrow still accounted for a small percentage (Supplemental Figure 4, A and B). The absence of PSGL1^{lo}CD4$^+$ T cells in the blood circulation and their CD62L$^-$CD44^{hi} T effector memory phenotype (Tem) suggested that they could be Trm cells. Trm cells are characterized by high expression of CD69, CD103, CXCR6, and P2RX7, but low expression of CCR7 and S1PR1 (21).

To test the hypothesis that PSGL1^{lo}CD4$^+$ T cells in cGVHD target tissues represent Trm cells, we compared the RNA-Seq profile of sorted splenic PSGL1^{lo}CD4$^+$ T cells from GVHD-free

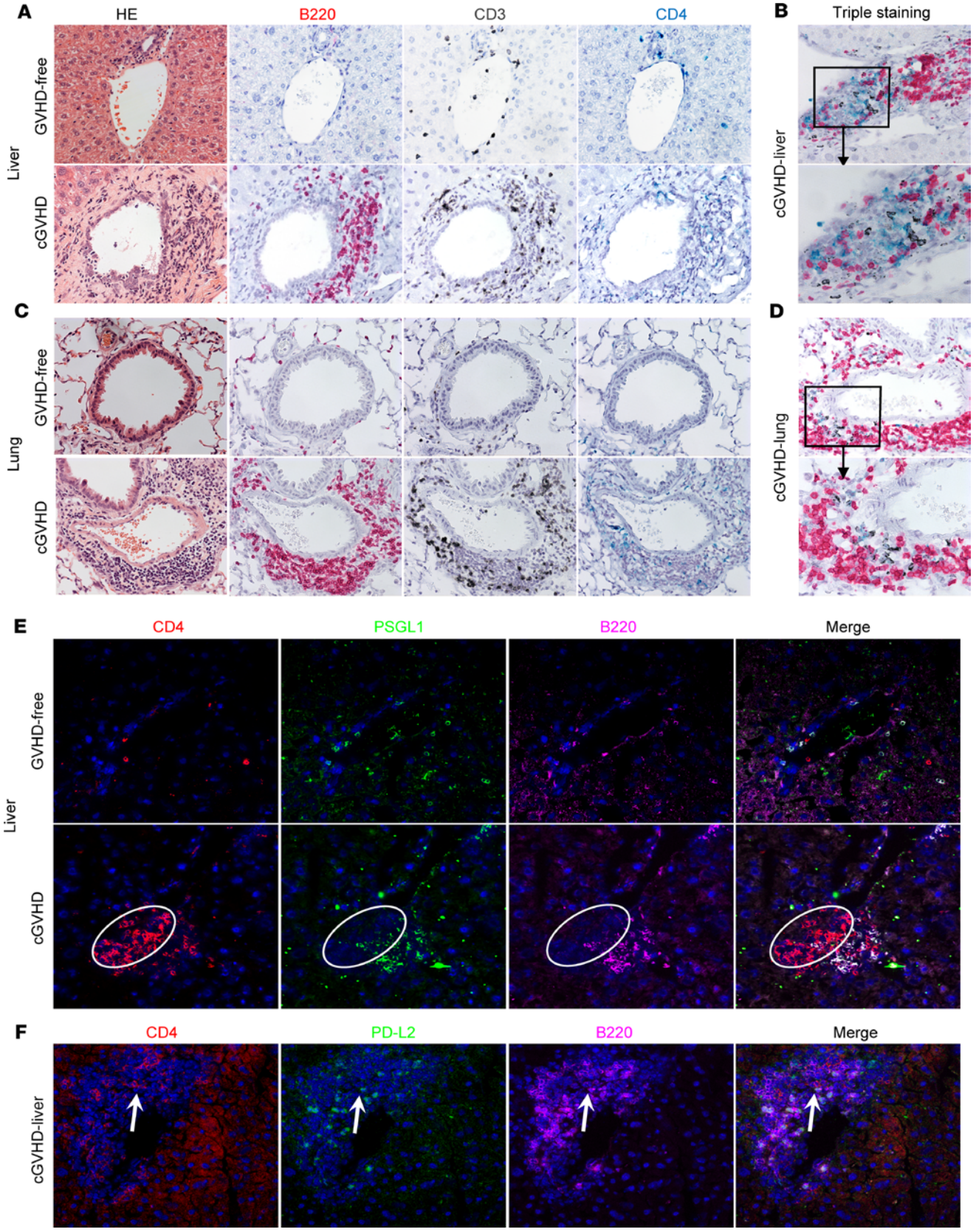

Figure 2. Adjoining PSGL1^{lo}CD4^{+} T cells and B cells are present in cGVHD target tissues. At 60 days after HCT, liver (**A** and **B**) and lung (**C** and **D**) tissues of recipients given C57BL/6 TCD-BM alone or with splenic Thy1.2 T cells were stained with IHC for B220, CD3, and CD4 separately or together (original magnification, ×400; **B** and **D** bottom panel original magnification, ×630). (**E**) Liver sections were also stained with immunofluorescent mAb for CD4, PSGL1, and B220. The oval demarcates a region of accumulated PSGL1^{lo}CD4^{+}T cells that colocalize with B220^{+} B cells. (**F**) Liver sections were stained with antibodies against CD4, PD-L2, and B220. Arrows show PD-L2^{+} B cells adjacent to CD4^{+} cells (**E** and **F**, original magnification, ×200). One representative experiment of 4 replicates is shown.

and cGVHD recipients at 30 days after HCT. PSGL1^{lo}CD4$^+$ T cells from cGVHD recipients expressed typical Trm markers, with high expression of mRNA for *Cd69*, *Cxcr6*, *P2rx7*, and *Il7ra* and low expression of mRNA for *Ccr7*, *S1pr1*, *Klrg1*, and *Klf2*, although we found little difference in expression of *Cd49a* compared with PSGL1^{lo}CD4$^+$ T cells from GVHD-free recipients (Figure 1C). Flow cytometry validated that PSGL1^{lo}CD4$^+$ T cells from cGVHD recipients had high expression of CD69, CXCR6, and P2RX7 and low expression of CCR7, with little difference in CD49a expression (Figure 1D and Supplemental Figure 5). These results indicated that PSGL1^{lo}CD4$^+$ T cells in cGVHD target tissues were Trm cells derived predominantly from mature T cells in the graft.

PSGL1^{lo}CD4$^+$ T cells are PD1^{hi}CXCR5$^-$ B cell helpers. Our previous studies suggested that extrafollicular PSGL1^{lo}CD4$^+$ T cells in GVHD target tissues might have a B cell helper function because the absence of PSGL1^{lo}CD4$^+$ T cells in the recipients was associated with reduction of anti-dsDNA autoantibodies (20). Consistently, in the current studies, with IHC staining and immunofluorescent staining, we observed apposed CD4$^+$ T cells and B cells in the liver and lung tissues of cGVHD recipients, but only scattered CD4$^+$ T cells and B cells in the tissues of GVHD-free recipients (Figure 2, A–D). We also observed PSGLl$^{lo/-}$CD4$^+$ T cells apposed with PSGL1$^{hi/+}$ B cells (Figure 2E). Many B cells juxtaposed to the CD4$^+$ T cells appeared to be PD-L2$^+$ memory B cells (Figure 2F). These results suggest that PSGL1^{lo}CD4$^+$ T cells interacted with B220$^+$ B cells and PD-L2$^+$ memory B cells in the target tissues of cGVHD mice.

We compared gene expression and cell surface receptor profiles of PSGL1^{lo} and PSGL1^{hi}CD4$^+$ T cells from cGVHD mice. PSGL1^{lo}CD4$^+$ T cells and PSGL1^{hi}CD4$^+$ T cells in the spleen, liver, and lung had numerous differentially expressed genes (Figure 3, A and B). In at least 2 of the 3 organs, PSGL1^{lo}CD4$^+$ T cells had high expression levels of genes for surface receptors related to T cell–B cell interactions, including *Pd1*, *Icos*, *Cd40l*, *Slamf6*, and *Cxcr5*, and low expression levels of genes for surface markers related to anergy/exhaustion, including *Tim3* and *Lag3* (Figure 3C). They also had high expression levels of genes for nuclear factors *Maf*, *Stat3*, and *Bcl6*, but low expression levels of genes for *Eomes* and *T-bet*. They had high expression levels of genes for *Il2*, *Cxcl13*, and *Il21*, but low expression levels of genes for *Ifng* (Figure 3C). Differential expression levels of proteins for surface receptors (i.e., PD1, ICOS, CD40L, and SLAMF6), nuclear factors (i.e., MAF), and cytokines (i.e., IL-21, IFNγ, and IL-13) were validated by flow cytometry (Figure 3, D–F; and Supplemental Figure 6, A–D).

Although the general gene expression profiles of PSGL-1^{lo}CD4$^+$ T cells from the spleen, liver, and lung appeared to be similar (Figure 3C), a more in-depth analysis showed that the PSGL1^{lo}CD4$^+$ T cells from GVHD target tissues of the liver and lung had high activation of KEGG pathways, such as cytokine-cytokine receptor interaction pathway and graft-versus-host disease pathway, as compared with PSGL1^{lo}CD4$^+$ T cells from the spleen (Supplemental Figure 6, E–G). In cGVHD recipients, PSGL1^{lo}CD4$^+$ T cells from the liver had higher expression of chemokine receptors such as Ccr5, Cxcr3, and Cxcr6 than those from the spleen (Supplemental Figure 6G), consistent with our previous report that donor T cell migration into different tissues is guided by their expression of chemokine receptors and corresponding chemokines from the target tissues (25).

Since Tfh cells from the spleen of GVHD-free recipients were also mostly PSGL1^{lo} (Supplemental Figure 7), we compared PSGL-1^{lo}CD4$^+$ T cells with the Tfh cells as well as with PSGL1^{hi} and naive CD4$^+$ T cells. We found that PSGL1^{lo}CD4$^+$ T cells expressed lower levels of PD1, ICOS, SLAMF6, and MAF than Tfh cells; in contrast, compared with PSGL1^{hi}CD4$^+$ T cells, PSGL1^{lo}CD4$^+$ T cells expressed significantly higher levels (Figure 3, D and E; and Supplemental Figure 6, A and B). Although PSGL1^{lo}CD4$^+$ T cells from cGVHD recipients had higher expression levels for *Pd1* and *Cxcr5* mRNA compared with PSGL1^{hi}CD4$^+$ T cells, they had only higher expression levels of PD1, with little expression of CXCR5, as measured by flow cytometry (Figure 3, C and D; and Supplemental Figure 6A). Although PSGL1^{lo}CD4$^+$ T cells had higher expression levels of PD1, they had lower expression levels of other anergy/exhaustion markers such as LAG3 and TIM3 and lower expression levels of the terminal differentiation marker KLRG1 and the T cell marker IL-7R (Figure 3G). Therefore, consistent with a report that PD1 expression level alone is not associated with alloreactive T cell anergy/exhaustion status (26), these results suggest that PSGL1^{lo}CD4$^+$ T cells had a PD1^{hi} CXCR5$^-$ phenotype of extrafollicular B cell helpers.

PD1 deficiency in donor T cells leads to expansion of PSGL-1^{lo}CD4$^+$ T cells but reduction of autoantibody production. The role of PD1 expression by Tfh cells and its interaction with PD-L2 expression by B cells is known to be important during T cell–B cell interaction in GCs (6), but it remains unclear during extrafollicular T cell–B cell interaction, especially in nonlymphoid tissues. Therefore, we tested whether PD1 expressed by PSGL-1^{lo}CD4$^+$ T cells plays an important role in their interaction with B cells. Because of lack of mice with specific PD1 deficiency in T cells, we used PD1$^{-/-}$ C57BL/6 donors. Consistent with previous reports (27), PD1 deficiency in donor T cells markedly enhanced acute GVHD with different doses of donor spleen cells. The long-term survival was similar in recipients given 0.0625×10^6 PD1$^{-/-}$ donor Thy1.2$^+$ T cells and in recipients given 0.25×10^6 WT donor Thy1.2$^+$ T cells, and approximately half of the recipients survived up to 60 days in both groups with clinical signs of cGVHD such as weight loss and hair loss (Supplemental Figure 8A). Because of the different donor T cell doses, we did not focus on clinical cGVHD severity in the 2 groups. Instead, we focused on changes in histopathology and percentages of PSGL1^{lo}CD4$^+$ T cells, naive B cells, memory B cells, and plasma cells in the spleen and the liver tissues, as well as total IgG and anti–dsDNA IgG concentrations in the serum.

We observed that recipients given PD1$^{-/-}$ donor T cells had more lymphocyte infiltration in the liver tissue, but less damage in the skin and salivary gland, and no significant difference in the lung (Supplemental Figure 8B). The recipients given PD1$^{-/-}$ donor T cells also had less collagen deposition in the skin and salivary gland, although no obvious difference in the liver or lung (Supplemental Figure 8C). Additionally, the recipients given PD1$^{-/-}$ T cells appeared to have less IgG deposition in the liver and skin tissues (Supplemental Figure 8D).

The yield of PSGL1^{lo}CD4$^+$ T cells in the spleen and liver of recipients given PD1$^{-/-}$ donor T cells was higher than that of recipients

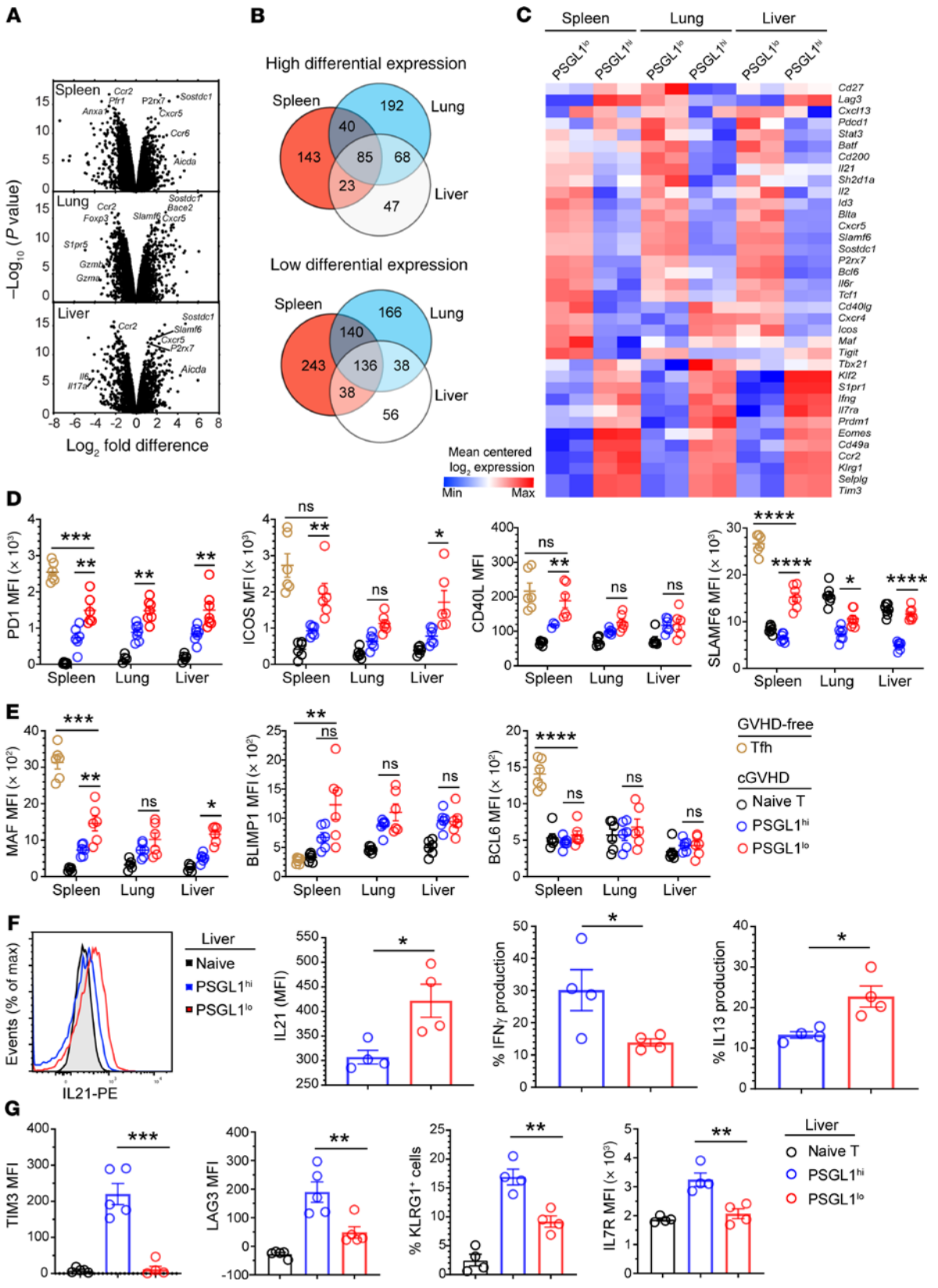
A
Spleen
Lung
Liver
Ccr2
Pfr1
P2rx7
Sostdc1
Anxa1
Cxcr5
Ccr6
Aicda
Bace2
Foxp3
Slamf6
S1pr5
Gzmb
Gzma
Il6
Il17a
−Log10 (P value)
Log2 fold difference
B
High differential expression
Spleen
Lung
Liver
192
40
143
85
68
23
47
Low differential expression
166
140
243
136
38
38
56
C
Spleen
Lung
Liver
PSGL1lo
PSGL1hi
Cd27
Lag3
Cxcl13
Pdcd1
Stat3
Batf
Cd200
Il21
Sh2d1a
Il2
Id3
Blta
Cxcr5
Slamf6
Sostdc1
P2rx7
Bcl6
Il6r
Tcf1
Cd40lg
Cxcr4
Icos
Maf
Tigit
Tbx21
Klf2
S1pr1
Ifng
Il7ra
Prdm1
Eomes
Cd49a
Ccr2
Klrg1
Selplg
Tim3
Mean centered log2 expression
Min
Max
D
PD1 MFI (× 10³)
ICOS MFI (× 10³)
CD40L MFI
SLAMF6 MFI (× 10³)
ns
Spleen
Lung
Liver
E
MAF MFI (× 10²)
BLIMP1 MFI (× 10²)
BCL6 MFI (× 10²)
GVHD-free
Tfh
cGVHD
Naive T
PSGL1hi
PSGL1lo
F
Events (% of max)
IL21-PE
Liver
Naive
PSGL1hi
PSGL1lo
IL21 (MFI)
% IFNγ production
% IL13 production
G
TIM3 MFI
LAG3 MFI
% KLRG1+ cells
IL7R MFI (× 10³)
Liver
Naive T
PSGL1hi
PSGL1lo

Figure 3. Tissue-resident PSGL^{lo}CD4$^+$ T cells are B cell helpers. PSGL1^{lo} and PSGL1^{hi} CD62L$^-$ CD4$^+$ T cells from the spleen, lung, and liver of cGVHD recipients were sorted for RNA sequencing at 30 days after HCT. (**A**) Volcano plot of all gene expression levels between PSGL1^{hi} and PSGL1^{lo} CD4$^+$ T cells. (**B**) Numbers of genes with high and low differential expression in PSGL1^{lo}CD4$^+$ T cells compared with PSGL1^{hi}CD4$^+$ T cells. (**C**) The heatmap analysis of clustered genes related to B cell helper features by PSGL1^{hi} and PSGL1^{lo} CD4$^+$ T cells. (**D**) Surface expression levels of PD1, ICOS, CD40L, and SLAMF6 among naive CD4$^+$ T cells, Tfh cells, PSGL1^{lo} T cells and PSGL1^{hi} CD4$^+$ T cells. (**E**) Intracellular expression levels of MAF, BLIMP1, and BCL6. (**F**) Sorted PSGL1^{lo}CD4$^+$ T cells from the liver tissue were stained for intracellular IL-21, IFNγ, and IL-13. Mean ± SEM of MFI is shown for IL-21, and percentages for IFNγ$^+$ and IL-13$^+$ cells. (**G**) Surface expression of T cell anergy/exhaustion-related receptors TIM3, LAG3, KLRG1, and IL-7R. Mean ± SEM of MFI is shown, N = 4–7 combined from at least 2 replicate experiments. P values were calculated by unpaired 2-tailed Student's t tests (**D**–**F**) or 1-way ANOVA multiple-comparisons test (**G**). *P < 0.05; **P < 0.01; ***P < 0.001; ****P < 0.0001.

given WT donor T cells (Figure 4A). The CD19$^{lo/-}$CD138$^+$ plasma cells, CD19$^+$IgD$^+$CD80$^-$ naive B cells, and CD19$^+$IgD$^-$CD80$^+$PD-L2$^+$ memory B cells were gated, as shown in Supplemental Figure 8E. As compared with recipients given WT T cells, the recipients given PD1$^{-/-}$ T cells had no significant difference in the percentage of naive or memory B cells in the spleen and liver, but had a significant increase in the spleen and slight decrease in the percentage of CD19$^{lo/-}$CD138$^+$ plasma cells in the liver (Figure 4B). In addition, the plasma cells in the spleen and liver of recipients given PD1$^{-/-}$ donor T cells had higher expression of Blimp-1 and IRF-4 (Supplemental Figure 8F), suggesting that they are IgG–producing cells, as previously reported (28). Although total serum IgG concentrations were not different between the 2 groups, the serum concentrations of anti–dsDNA IgG were significantly lower in recipients given PD1$^{-/-}$ donor T cells (Figure 4C).

The lack of obvious reduction in the percentage of plasma cells in the liver of recipients given PD1$^{-/-}$ T cells might result from augmented GVHD induced by PD1$^{-/-}$ T cells. Consistent with this notion, the liver of recipients given PD1$^{-/-}$ TCD-BM alone contained higher percentages of memory B cells, but lower percentages of plasma cells compared with recipients given WT-TCD-BM alone (Supplemental Figure 8G). These results suggest that PD1 expression by PSGL1^{lo}CD4$^+$ T cells was required for specific augmentation of anti–dsDNA IgG autoantibody production in cGVHD recipients. These results also suggest that PD1 expressed by PSGL1^{lo}CD4$^+$ T cells may have augmented plasma cell expansion and autoantibody production in GVHD target tissues.

PD-L2 deficiency in donor B cells and other myeloid cells leads to expansion of PSGL1^{lo}CD4$^+$ T cells but reduction of autoantibody production. We also tested whether PSGL1^{lo}CD4$^+$ T cell interaction with B cells requires expression of PD-L2 by B cells. Because of lack of mice with PD-L2 deficiency specifically in B cells, we used PD-L2$^{-/-}$ C57BL/6 TCD-BM to provide PD-L2$^{-/-}$ B cells. WT Thy1.2$^+$ (CD45.1$^+$, 0.25 × 10^6) were cotransplanted with TCD-BM (5 × 10^6) from WT (CD45.1$^+$) or PD-L2$^{-/-}$ (CD45.2$^+$) donors into lethal TBI-conditioned BALB/c recipients. As compared with recipients given WT-TCD-BM, recipients given PD-L2$^{-/-}$ TCD-BM showed slightly better survival (Supplemental Figure 9A). However, the recipients given PD-L2$^{-/-}$ TCD-BM cells showed less inflammation and damage in the lung, skin, and salivary gland, although not in the liver. Collagen deposition in the lung, skin, and salivary gland and IgG antibody deposition in the liver and skin were also lower in recipients given PD-L1$^{-/-}$ TCD-BM cells compared with those given WT cells (Supplemental Figure 9, B–D).

At 60 days after HCT, the percentage and yield of PSGL1^{lo}CD4$^+$ T cells were higher in the liver tissues, but not different in the spleen of recipients of PD-L2$^{-/-}$ BM compared with WT BM (Figure 4D). The CD19$^{lo/-}$CD138$^+$ plasma cells, CD19$^+$IgD$^+$CD80$^-$ naive B cells, and CD19$^+$IgD$^-$CD80$^+$ CD73$^+$ memory B cells were gated, as shown in Supplemental Figure 8E and Supplemental Figure 9E. The percentages of naive and memory B cells in the spleen and liver were not significantly different between the 2 groups, but plasma cells in the liver of recipients given PD-L2$^{-/-}$ BM were slightly reduced (Figure 4E). Both total IgG and anti–dsDNA IgG concentrations in the serum were significantly lower in the recipients of PD-L2$^{-/-}$ BM compared with WT BM (Figure 4F). Interestingly, recipients given WT T cells and WT or PD-L1$^{-/-}$ TCD-BM cells showed no significant difference in total serum IgG or anti–dsDNA IgG concentrations, although the percentages of PSGL1^{lo}CD4$^+$ T cells in the liver tissues were higher in recipients given PD-L1$^{-/-}$ BM compared with WT BM (Supplemental Figure 10, A–C). These results suggest that PD-L2 but not PD-L1 expression by donor B cells was required to augment total IgG and anti–dsDNA IgG autoantibody production in cGVHD recipients.

PSGL1^{lo}CD4$^+$ T cell interaction with B cells via PD1 and PD-L2 augments autoantibody production. In the experiments described above, PD-1 deficiency was not confined to PSGL1^{lo}CD4$^+$ T cells and PD-L2 deficiency was not confined to B cells. Therefore, we used adoptive transfer experiments to determine whether PSGL1^{lo}CD4$^+$ T cell PD1 interacts with B cell PD-L2 and regulates autoantibody production. As depicted in Figure 5A, sorted CD45.1$^+$PSGL1^{lo}CD4$^+$ T cells and CD45.1$^+$PSGL1^{hi}CD4$^+$ T cells (1 × 10^6) from the liver and lung of day 30 primary cGVHD recipients and sorted CD45.1$^+$PSGL1^{lo}CD4$^+$ T cells from the spleen of GVHD-free recipients were injected into GVHD-free adoptive BALB/c chimeras grafted with donor-type C57BL/6 WT TCD-BM cells. Adoptive recipients given PBS were used as an additional control. At day 14 after cell transfer, the adoptive recipients were analyzed for the presence of the adoptively transferred CD45.1$^+$ T cells in the spleen and liver, the percentage of plasma cells in the spleen and liver, and the serum concentration of total IgG and anti–dsDNA IgG.

The injected CD45.1$^+$PSGL1^{lo}CD4$^+$ T cells and CD45.1$^+$PSGL1^{hi}CD4$^+$ T cells were present in both the spleen and liver of the adoptive recipients, but they localized preferentially in the liver, especially with cells that originated from the liver and lung (Supplemental Figure 11 and Figure 5B). The numbers of CD45.1$^+$ T cells recovered from the spleen at day 14 after the adoptive transfer did not differ between recipients given non-GVHD or cGVHD PSGL1^{lo} cells or cGVHD PSGL1^{hi} cells. The numbers of CD45.1$^+$ T cells recovered from the liver at day 14 after the adoptive transfer were more than 2-fold higher in recipients given cGVHD PSGL1^{lo}CD4$^+$ T cells than in recipients given non-GVHD PSGL1^{lo}CD4$^+$ T cells. The numbers of CD45.1$^+$ T cells recovered from the liver did not differ between recipients given cGVHD PSGL1^{lo} or PSGL1^{hi} CD4$^+$ T cells (Figure 5B). These results indicated that PSGL1^{lo}CD4$^+$ T cells and PSGL1^{hi}CD4$^+$ T cells from cGVHD target tissues preferentially home back to the

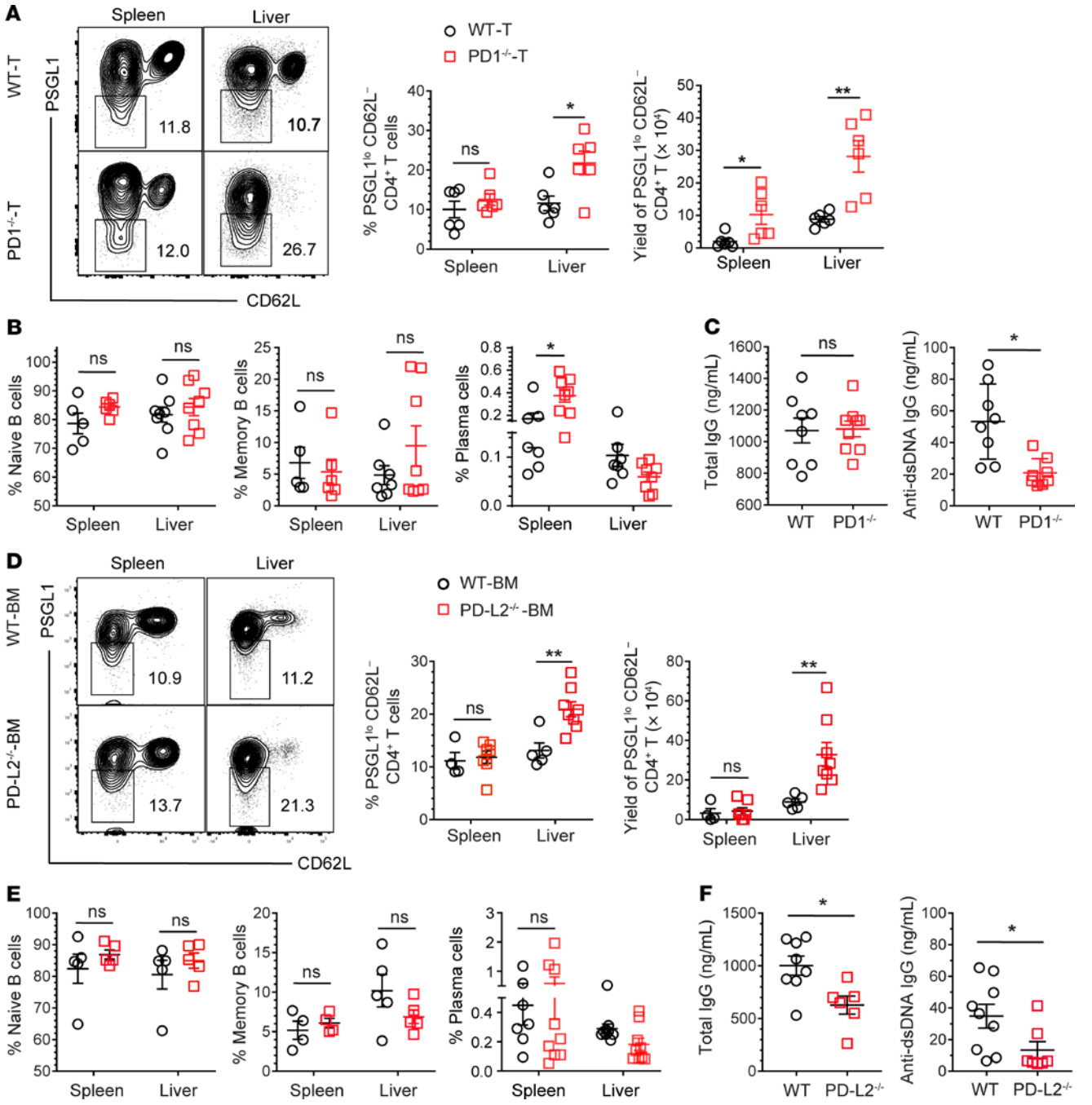

Figure 4. PD1 deficiency in T cells and PD-L2 deficiency in B cells enhances expansion of PSGL1^{lo}CD4$^+$ T cells in the liver but reduces autoantibody production. Lethally irradiated BALB/c mice received Thy1.2$^+$ T cells from PD1$^{-/-}$ donors and TCD-BM from WT donors (**A**–**C**) or Thy1.2$^+$ T cells from WT donors and TCD-BM from PD-L2$^{-/-}$ donors (**D**–**F**). At day 60 after HCT, recipients were evaluated for percentage of donor-type PSGL1^{lo}CD4$^+$ T cells among donor CD4$^+$ T cells, absolute numbers of donor-type PSGL1^{lo}CD4$^+$ T cells, and percentages of CD19$^+$IgD$^+$CD80$^-$ naive B cells, CD19$^+$IgD$^-$CD80$^+$PD-L2$^+$ and CD19$^+$IgD$^-$CD80$^+$CD73$^+$ memory B cells, and CD19$^{lo/-}$CD138$^+$ plasma cells among CD19$^+$ B cells in the spleen and liver. Mean ± SEM is shown, N = 5–8, combined from 2 independent experiments. (**A**) Percentage and yield of PSGL1^{lo}CD4$^+$ T cells in the recipients given WT or PD1$^{-/-}$ T cells. (**B**) Percentage of naive B, memory B, and plasma cells. (**C**) Serum total IgG and anti-ds DNA IgG autoantibody concentration detected by ELISA. (**D**) Percentages and yield of PSGL1^{lo}CD4$^+$ T cells in the recipients given WT T cells or PD-L2$^{-/-}$ TCD-BM cells. (**E**) Percentage of naive B, memory B, and plasma cells. (**F**) Serum concentrations of total IgG and anti–dsDNA IgG autoantibodies. P values were calculated by 1-way ANOVA multiple-comparisons test (**A**, **B**, **D**, **E**) and unpaired 2-tailed Student's t tests (**C** and **F**). *P < 0.05; **P < 0.01; ***P < 0.001.

GVHD target tissues after transfer into adoptive recipients.

As compared with controls given PBS, injection of PSGL-1^{lo}CD4$^+$ T cells or PSGL1^{hi}CD4$^+$ T cells did not change the percentage of plasma cells in the spleen of adoptive recipients. Injection of non-GVHD and cGVHD PSGL1^{lo}CD4$^+$ T cells increased the percentage of plasma cells in the liver, whereas injection of cGVHD PSGL1^{hi}CD4$^+$ T cells had no effect (Figure 5C). Similarly, injection of non-GVHD and cGVHD PSGL1^{lo}CD4$^+$ T cells

increased serum concentrations of total IgG and anti–dsDNA IgG, whereas injection of PSGL1^{hi}CD4$^+$ T cells had no effect (Figure 5D). These results indicated that PSGL1^{lo}CD4$^+$ T cells but not PSGL1^{hi}CD4$^+$ T cells from cGVHD target tissues augmented B cell differentiation to plasma cells and increased the production of IgG and anti-dsDNA autoantibodies.

To evaluate the role of PD-L2 expression by B cells interacting with PSGL1^{lo}CD4$^+$ T cells, CD45.1$^+$PSGL1^{lo}CD4$^+$ T cells from the liver and lung of primary cGVHD recipients were transferred into adoptive BALB/c chimeras grafted with C57BL/6 WT TCD-BM (WT chimeras) or PD-L2$^{-/-}$ TCD-BM (PD-L2$^{-/-}$ chimeras) (Figure 5E). The numbers of CD45.1$^+$ T cells recovered from the spleen at day 14 were lower in the PD-L2$^{-/-}$ chimeras than in WT chimeras, but the numbers of cells recovered from the liver did not show a statistically significant difference (Figure 5F). In WT chimeras, injection of PSGL-1^{lo}CD4$^+$ T cells increased the percentage of plasma cells in the liver and increased the serum concentrations of IgG and anti–dsDNA IgG. But in PD-L2$^{-/-}$ chimeras, injection of PSGL1^{lo}CD4$^+$ T cells did not increase either the percentage of plasma cells or the serum concentrations of IgG or anti–dsDNA IgG (Figure 5, G and H). These results indicated that augmentation of B cell differentiation and IgG antibody production by PSGL1^{lo}CD4$^+$ T cells required B cell expression of PD-L2.

To evaluate the role of PD1 expression by PSGL1^{lo}CD4$^+$ T cells, sorted WT or PD1$^{-/-}$ PSGL1^{lo} CD4$^+$ T cells from the liver and lung of primary recipients were transferred into adoptive BALB/c chimeras grafted with C57BL/6 TCRβ$^{-/-}$TCD-BM cells (Figure 5I). The use of TCRβ$^{-/-}$TCD-BM was to avoid the influence of BM-derived T cells. Again, the injected PSGL1^{lo}CD4$^+$ T cells localized preferentially in the liver (Figure 5J). Injection of WT PSGL1^{lo}CD4$^+$ T cells increased the percentage of plasma cells in the liver and increased the serum concentrations of IgG and anti–dsDNA IgG. In contrast, injection of PD1$^{-/-}$ PSGL-1^{lo}CD4$^+$ T cells did not increase either the percentage of plasma cells or serum concentrations of IgG or anti–dsDNA IgG (Figure 5, K and L). These results indicated that augmentation of B cell differentiation and IgG antibody production by PSGL1^{lo}CD4$^+$ T cells in GVHD target tissues required their expression of PD1.

To evaluate the PD1 and PD-L2 interaction between PSGL-1^{lo}CD4$^+$ T cells and B cells, we supplemented the in vivo results with in vitro culture experiments. Sorted CD19$^+$IgD$^+$CD80$^-$ naive B cells and CD19$^+$IgD$^-$CD80$^+$PD-L2$^+$ memory B cells (2×10^4 to 5×10^4 cells/well) from the spleen of TCD-BM recipients were cocultured with PSGL1^{lo}CD4$^+$ T cells (0.4×10^4 to 1×10^4 cells/well) from the liver and lung tissues of cGVHD recipients at a 5:1 ratio for 4 days in the presence of anti-PD1, anti–PD-L2, or isotype control. PSGL1^{lo}CD4$^+$ T cells augmented IgG production by memory B cells but not naive B cells. The augmentation of IgG production by PSGL1^{lo}CD4$^+$ T cells was blocked both by anti-PD1 and by anti–PD-L2 mAb (Supplemental Figure 12, A and B). These results indicated that PSGL1^{lo}CD4$^+$ T cell augmentation of IgG production of memory B cells required direct PD1 interaction with PD-L2.

Peripheral blood T cells give rise to PD1^{hi}PSGL1^{lo} Trm cells in murine cGVHD recipients. Since almost all CD4$^+$ T cells among PBMCs in donors and recipients were PSGL1^{hi}, with few PSGL1^{lo}CD4$^+$ T cells (Figure 1 and Supplemental Figure 3), we tested whether murine PBMCs give rise to PSGL1^{lo}CD4$^+$ Trm cells in GVHD target organs. PBMCs (0.5×10^6, ~0.15×10^6 to 0.2×10^6 T cells) and TCD-BM cells (5×10^6) from C57BL/6 donors were injected into lethal TBI-conditioned BALB/c mice. Recipients given TCD-BM alone were used as controls. The recipients given PBMCs developed both acute and chronic GVHD as indicated by body weight loss and some early deaths (Figure 6A). Recipients that survived for more than 60 days developed typical cGVHD histopathology in the liver, lung, skin, and salivary gland (Figure 6B). As compared with GVHD-free recipients given TCD-BM alone, cGVHD recipients had higher percentages of PSGL1^{lo}CD4$^+$ T cells in the spleen, liver, and lung (Figure 6C), and most of them expressed high levels of PD1, ICOS, and tissue-resident markers, including CD69 and CXCR6 (Figure 6D). These results indicated that PSGL1^{hi}CD4$^+$ T cells among PBMCs can give rise to PSGL1^{lo}CD4$^+$ T cells in GVHD target tissues of MHC-mismatched recipients.

PSGL1^{hi}CD4$^+$ T cell differentiation into PSGL1^{lo}CD4$^+$ T cells in cGVHD recipients is IL-6R/Stat3 pathway dependent. We previously reported that PSGL1^{lo}CD4$^+$ T cell expansion in cGVHD recipients was Stat3-dependent (20), but it remains unknown whether PSGL1^{hi}CD4$^+$ T cell differentiation into PSGL1^{lo}CD4$^+$ T cells is also Stat3 dependent. To answer this question, we transplanted PBMCs containing nearly 100% PSGL1^{hi} T cells (0.5×10^6, ~0.15×10^6 to 0.20×10^6 T cells) from CD45.2$^+$ WT or Stat3$^{-/-}$ donors together with CD45.1$^+$ TCD-BM cells (5×10^6) from WT donors into lethal TBI-conditioned BALB/c recipients. The recipients given PBMCs from WT donors developed acute and chronic GVHD with weight loss and approximately 70% (10/15) survived for more than 40 days; in contrast, the recipients given PBMCs from Stat3$^{-/-}$ PBMCs showed little signs of GVHD, and 100% (10/10) survived for more than 40 days (Figure 7A). The percentages of PSGL^{lo}CD4$^+$ T cells among the injected CD45.2$^+$ donor T cells in the spleen, liver, and lung at 40 days after HCT were lower with Stat3$^{-/-}$ T cells than with WT T cells (Figure 7B). These results indicated that Stat3 promoted the differentiation of PSGL1^{hi}CD4$^+$ T cells into PSGL1^{lo}CD4$^+$ T cells.

IL-6R signaling activates the Stat3 signaling pathway (29). Blockade of IL-6R signaling by anti–IL-6R mAbs ameliorates GVHD in murine models and in humans with concomitant expansion of Treg cells (30, 31). We tested whether blockade of IL-6R signaling by anti–IL-6R could regulate PSGL1^{hi}CD4$^+$ T cell differentiation into PSGL1^{lo}CD4$^+$ T cells. Accordingly, lethal TBI-conditioned BALB/c recipients were grafted with CD45.2$^+$ PBMCs and CD45.1$^+$ TCD-BM. The recipients were treated with anti–IL-6R mAb or control rat IgG (500 μg/mouse) from days 1 and 0 and then weekly for 4 weeks. Anti–IL-6R mAb treatment reduced the severity of GVHD as indicated by lower loss of body weight (Figure 7C). Anti–IL-6R treatment also significantly reduced the percentage of PSGL1^{lo}CD4$^+$ T cells among the injected donor CD4$^+$ T cells in the liver and lung, but not in the spleen (Figure 7D). Taken together, these results showed that the IL-6R/Stat3 signaling pathway promoted PSGL1^{hi}CD4$^+$ T cell differentiation into PSGL^{lo}CD4$^+$ T cells in cGVHD target tissues.*Human peripheral blood T cells give rise to PD1^{hi}PSGL1^{lo}CD4$^+$ Trm cells that interact with B cells in the GVHD target tissues in humanized recipients*. We tested whether human PSGL1^{hi}CD4$^+$ T cells gave rise to PSGL1^{lo}CD4$^+$ T cells using a humanized

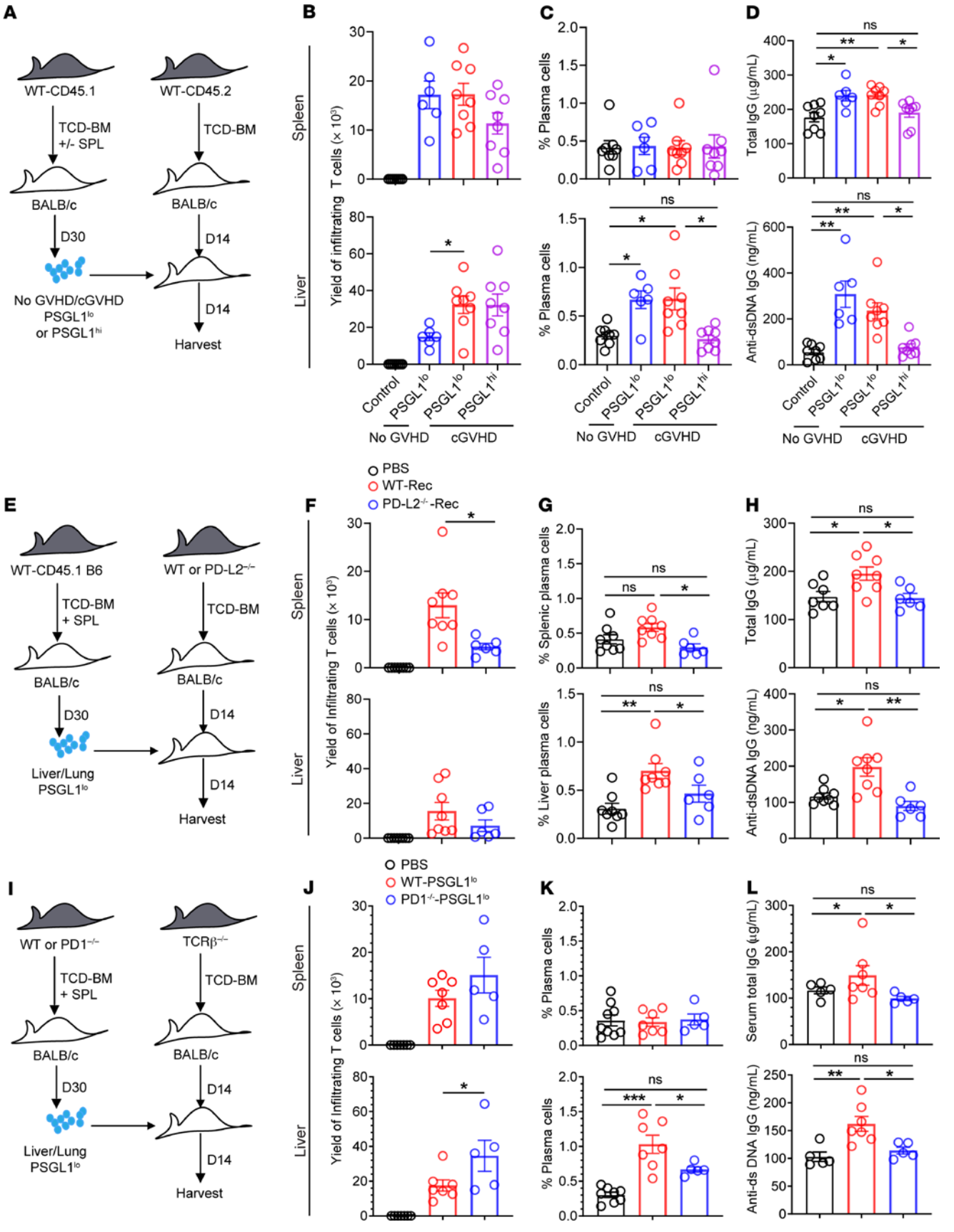

J Clin Invest. 2021;131(1):e135468 https://doi.org/10.1172/JCI135468

Figure 5. PSGL1^{lo}CD4$^+$ T cell PD1 interaction with B cell PD-L2 augments B cell differentiation to plasma cells and IgG autoantibody production in adoptive transfer recipients. cGVHD was induced in BALB/c recipients by transplanting CD45.1$^+$ TCD-BM alone or together with splenocytes from C57BL/6 donors. At 30 days after HCT, donor-type PSGL1^{lo}CD62L$^-$CD4$^+$ T cells and PSGL1^{hi}CD62L$^-$CD4$^+$ T cells were sorted and adoptively transferred into irradiated BALB/c chimeras grafted with TCD-BM from C57BL/6 WT donors 14 days previously. At 14 days after the adoptive transfer, numbers of the injected PSGL1^{lo}CD62L$^-$CD4$^+$ T cells and percentages of CD19$^{lo/-}$CD138$^+$ plasma cells among total donor CD19$^+$ B cells in the spleen and liver were analyzed, and serum concentrations of total IgG and anti–dsDNA IgG were measured. Mean ± SEM is shown, N = 5–8 combined from at least 2 replicate experiments. (**A**–**D**) Transfer of GVHD-free spleen-derived PSGL1^{lo}CD62L$^-$ cells, GVHD liver- and lung-derived PSGL1^{lo}CD62L$^-$ or PSGL1^{hi}CD62L$^-$ CD4$^+$ T cells into adoptive recipients with WT B cells. (**E**–**H**) Transfer of WT PSGL1^{lo}CD62L$^-$ CD4$^+$ T cells into adoptive recipients with WT or PD-L2$^{-/-}$ B cells. (**I**–**L**) Transfer of WT or PD1$^{-/-}$ PSGL1^{lo}CD62L$^-$ CD4$^+$ T cells into adoptive recipients with WT B cells. P values were calculated by 1-way ANOVA multiple-comparisons test (**C**, **G**, **K**) or multiple t tests (**B**, **D**, **F**, **H**, **J**, **L**). $^*P < 0.05$; $^{**}P < 0.01$; $^{***}P < 0.001$.

murine model, in which MHC I and II–deficient (MHC$^{-/-}$) NSG mice that expressed human HLA-A2 and HLA-DR4 (A2$^+$DR4$^+$ NSG) were used as recipients, and HLA-A2$^-$DR4$^-$ healthy volunteers were used as donors. A2$^-$DR4$^-$ PBMCs containing 12 × 10^6 T cells were injected into MHC$^{-/-}$HLA-A2$^+$DR4$^+$ NSG recipients or control MHC$^{-/-}$ NSG recipients. Whereas MHC$^{-/-}$ NSG recipients showed little signs of GVHD and appeared to be healthy, the A2$^+$DR4$^+$ NSG recipients developed severe GVHD with body weight loss and hair loss, although they all survived for more than 60 days (Figure 8A). The HLA-A2$^+$DR4$^+$ cGVHD recipients showed inflammatory infiltration; human IgG deposition; collagen deposition in the liver, lung, skin, and salivary glands; and high serum concentrations of anti–dsDNA human IgG. In contrast, MHC$^{-/-}$ recipients showed some infiltration, but little human IgG or collagen deposition in the tissues and low serum concentrations of anti–dsDNA human IgG (Figure 8, B–D; and Supplemental Figure 13A). These results indicate that HLA-A2$^-$DR4$^-$ human PBMCs can induce autoimmune-like cGVHD in humanized MHC$^{-/-}$HLA-A2$^+$DR4$^+$ NSG recipients.

PSGL1^{lo}CD4$^+$ T cells were not present among PBMCs of A2$^+$DR4$^+$ NSG recipients with cGVHD, but 10%–20% of PSGL1^{lo}CD4$^+$ T cells were present among donor CD4$^+$ T cells in the spleen, liver, and lung (Figure 8E), and most of them expressed markers of Trm, including high expression of CD69 and low expression of CCR7 and no difference in CD103 expression, as compared with PSGL1^{hi}CD4$^+$ T cells (Figure 8F). In addition, PSGL1^{lo}CD4$^+$ T cells had high expression of PD1, ICOS, and Tigit but not CXCR5 (Figure 8G). Finally, the PSGL-1^{lo}CD4$^+$ T cells in the liver produced IFN-γ and IL-21 and expressed CD40L (Supplemental Figure 13B). Taken together, these results indicated that PSGL1^{lo}CD4$^+$ T cells derived from human peripheral blood T cells in GVHD target tissues of a humanized murine model were tissue-resident T cells with B cell helper potential.

Human PSGL1^{lo}CD4$^+$ T cells augment autologous memory B cell differentiation into plasma cells in a PD1/PD-L2–dependent manner. To evaluate whether experiments with murine cells are relevant for human cells, we tested whether PSGL1^{lo}CD4$^+$ T cells interact with B cells in humanized NSG recipients given whole human PBMCs containing approximately 12% CD19$^+$ B cells and approximately 45% T cells (Supplemental Figure 14A). At day 60, donor B cells were hardly detectable in the blood, liver, or lung tissues of control MHC$^{-/-}$ NSG recipients. Only approximately 0.5% CD19$^+$ B cells were detected among splenic mononuclear cells, and most of them were CD27$^-$CD38$^-$ "naive" B cells (Supplemental Figure 14B). On the other hand, CD19$^+$ B cells could be detectable in the blood, spleen, liver, and lung tissues of HLA-A2$^+$DR4$^+$ humanized NSG recipients with cGVHD. In the blood, approximately 80% of the B cells had a CD27$^-$CD38$^-$ "naive" phenotype, approximately 20% had a CD27$^+$CD38$^-$ memory B phenotype, and none had a CD27$^+$CD38$^+$ plasmablast phenotype. In contrast, B cells in the spleen, liver, and lung contained 25%–50% CD27$^+$CD38$^-$ memory B cells and 6%–8% CD27$^+$CD38$^+$ plasmablasts (Supplemental Figure 14C). These results indicate that human B cells were activated and expanded in humanized A2$^+$DR4$^+$ NSG mice with cGVHD.

To evaluate the interaction between PSGL1^{lo}CD4$^+$ T cells and B cells in GVHD target tissues of humanized recipients, we used adjacent slides of formalin-fixed liver tissues to identify PSGL1^{lo}CD4$^+$ T cells and memory B cells by combination IHC staining of the following: 1) Maf (T cell marker), CD4, and CD20; 2) Maf, PSGL1, and PAX5 (B cell marker); 3) CD4, PAX5, and CD27 (marker for memory B and CD4$^+$ T cells) (Figure 9A). Because we observed that like other B cell helpers, PSGL1^{lo}CD4$^+$ T cells expressed higher levels of MAF (Figure 3E), we calculated the numbers of MAF$^+$CD4$^+$ or MAF$^+$PSGL1$^{lo/-}$ T cells that were juxtaposed with B cells. The numbers of MAF$^+$CD4$^+$ T cells colocalizing with CD20$^+$ B cells and the numbers of MAF$^+$PSGL1^{lo}/$^-$ T cells colocalizing with PAX5$^+$PSGL1$^+$ B cells in the tissue were markedly higher than in control MHC$^{-/-}$ NSG recipients without cGVHD (Figure 9B). This was also consistent with flow cytometry analysis that many donor B cells were present in the liver of humanized cGVHD mice, but few donor B cells were present in the liver of control mice (Supplemental Figure 14, B and C). Taken together, human PSGL1^{lo}CD4$^+$ T cells derived from PBMC PSGL1^{hi}CD4$^+$ T cells interacted with memory B cells in the liver tissue of humanized cGVHD recipients.

To directly evaluate the interactions of human PSGL1^{lo}CD4$^+$ T cells with autologous B cells, sorted human PSGL1^{lo}CD4$^+$ T cells from GVHD target tissues, including the spleen, liver, and lung of humanized HLA-A2$^+$DR4$^+$ NSG mice, were cocultured in vitro with sorted CD3$^-$CD19$^+$CD38$^{lo/-}$CD27$^-$ naive or CD3$^-$CD19$^+$CD38$^-$CD27$^+$ memory B cells from the same human PBMCs that were cryopreserved in liquid nitrogen when we performed the primary transfer experiments. Sorting of naive and memory B cells is depicted in Supplemental Figure 15A. PSGL1^{lo}CD4$^+$ T cells did not augment naive B cell differentiation into CD138$^+$CD27$^+$ plasma cells (Figure 9C). In contrast, PSGL1^{lo}CD4$^+$ T cells significantly augmented memory B cell differentiation into CD27$^+$CD138$^+$ plasma cells (Figure 9D). Besides augmenting plasma cell expansion, PSGL1^{lo}CD4$^+$ T cells also augmented IgG production, and the effect was blocked by IL-21R Fc (Figure 9E). Finally, blocking anti-PD1 and anti–PD-L2 markedly reduced the yield of plasma cells in the culture (Figure 9F). As compared with naive B cells, human memory B cells expressed high levels of PD-L2 as indicated by the MFI of PD-L2 (Supplemental Figure 15B). These results indicated that human PSGL1^{lo}CD4$^+$ T cells from GVHD target tissues of humanized murine recipients can augment autologous memory B

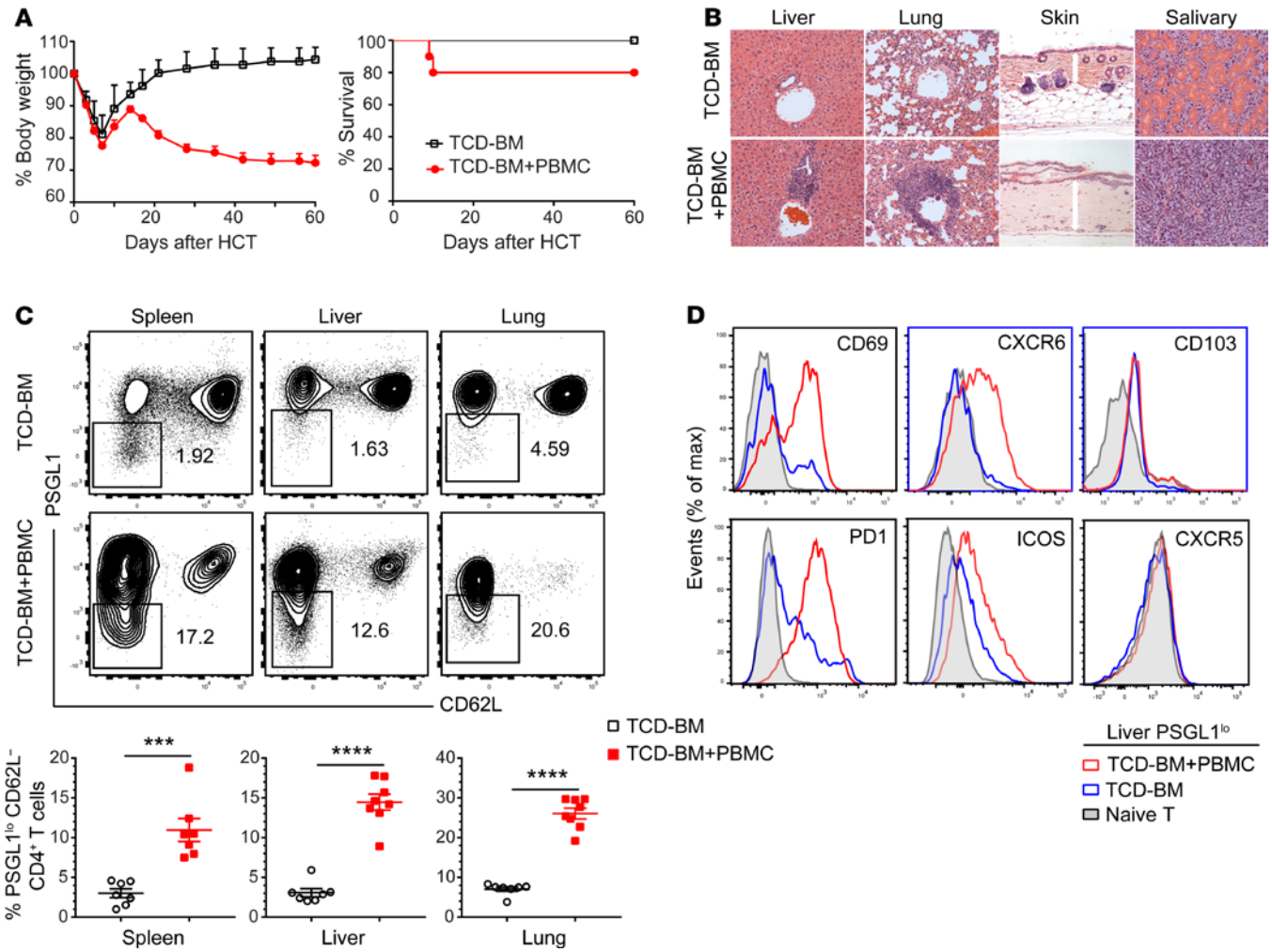

Figure 6. Donor PBMC PSGL1^{hi}CD4$^+$ T cells give rise to PSGL1^{lo}CD4$^+$ T cells in cGVHD recipients. cGVHD was induced in BALB/c recipients by transplanting PBMC and TCD-BM cells from C57BL/6 donors. At 60 days after HCT, donor-type T cells were analyzed for the percentage of PSGL1^{lo}CD62L$^-$CD4$^+$ T cells, which were further analyzed for expression of tissue-resident markers (CD69, CXCR6, and CD103) and B cell helper markers (PD1, ICOS, and CXCR5). (**A**) Curves of the survival percentage and percentage of body weight change. $N = 10$, combined from 2 replicate experiments. (**B**) H&E staining of liver, lung, skin, and salivary gland. One representative micrograph is shown of 6 in each group (original magnification, ×200). (**C**) Representative flow cytometry patterns of PSGL1 versus CD62L after gating on H-2b$^+$TCRβ$^+$CD4$^+$ T cells and mean ± SEM of percentage of PSGL1^{lo}CD62L$^-$CD4$^+$ T cells in the spleen, liver, and lung. $N = 7$. (**D**) Surface expression of CD69, CXCR6, CD103, PD1, ICOS, and CXCR5 among naive CD4$^+$ T cells from donors and PSGL1^{lo}CD62L$^-$CD4$^+$ T cells from GVHD-free recipients and from cGVHD recipients. One representative histogram is shown of 6 in each group. *P* values were calculated by unpaired 2-tailed Student's *t* tests. $^*P < 0.05$; $^{**}P < 0.01$; $^{***}P < 0.001$.

cell differentiation into plasma cells and augment their antibody production in a PD1- and PD-L2–dependent manner.

PDGL1^{lo}CD4$^+$ T cells appear to interact with memory B cells in GVHD target tissues of cGVHD patients. Next, we attempted to link our studies of PSGL1^{lo}CD4$^+$ T cell interaction with B cells in the mouse model and humanized mouse model to patients with cGVHD. Consistent with our studies using mouse and humanized mouse models (Figure 1 and Figure 8), PSGL1^{lo}CD4$^+$ T cells were undetectable among PBMCs of healthy human donors or cGVHD patients (Figure 10, A and B). Because we observed PSGL1^{lo}CD4$^+$ T cell and memory B cell interactions in the liver tissue of mouse and humanized mouse cGVHD recipients (Figure 2; and Figure 9, A and B), we tested whether similar interactions exist in the liver tissue of cGVHD patients.

Similar to IHC staining with formalin-fixed tissues in Figure 9A, we used 4 adjacent sections with the following staining combinations: 1) MAF (T cell marker), CD3, and CD20; 2) MAF, CD4, and CD20; 3) MAF, PSGL1, and PAX5 (B cell marker); 4) CD3, PAX5, and CD27 (marker for memory B cells and CD4$^+$ T cells) (Figure 10C). As shown in Figure 9, we used MAF staining to identify the potential PSGL1^{lo}CD4$^+$ T cells of the B cell helper. We observed that there were many T and B cells in the tissues (Figure 10C). We calculated the percentage of MAF$^+$ T cells that were juxtaposed with PAX5$^+$ B cells, and approximately 60%–80% of MAF$^+$ T cells were CD3$^+$, CD4$^+$, or PSGL1$^{lo/-}$, and approximately 20% of PAX5$^+$ B cells were CD27$^+$ memory B cells (Figure 10D). These observations suggest that an interaction between PSGL1$^{lo/-}$CD4$^+$ T cells and memory B cells existed in the liver tissue of cGVHD patients.

Discussion

Extrafollicular PSGL1^{lo}CD4$^+$ T cells that help B cell production of autoantibodies in lymphoid tissue of autoimmune SLE mice were

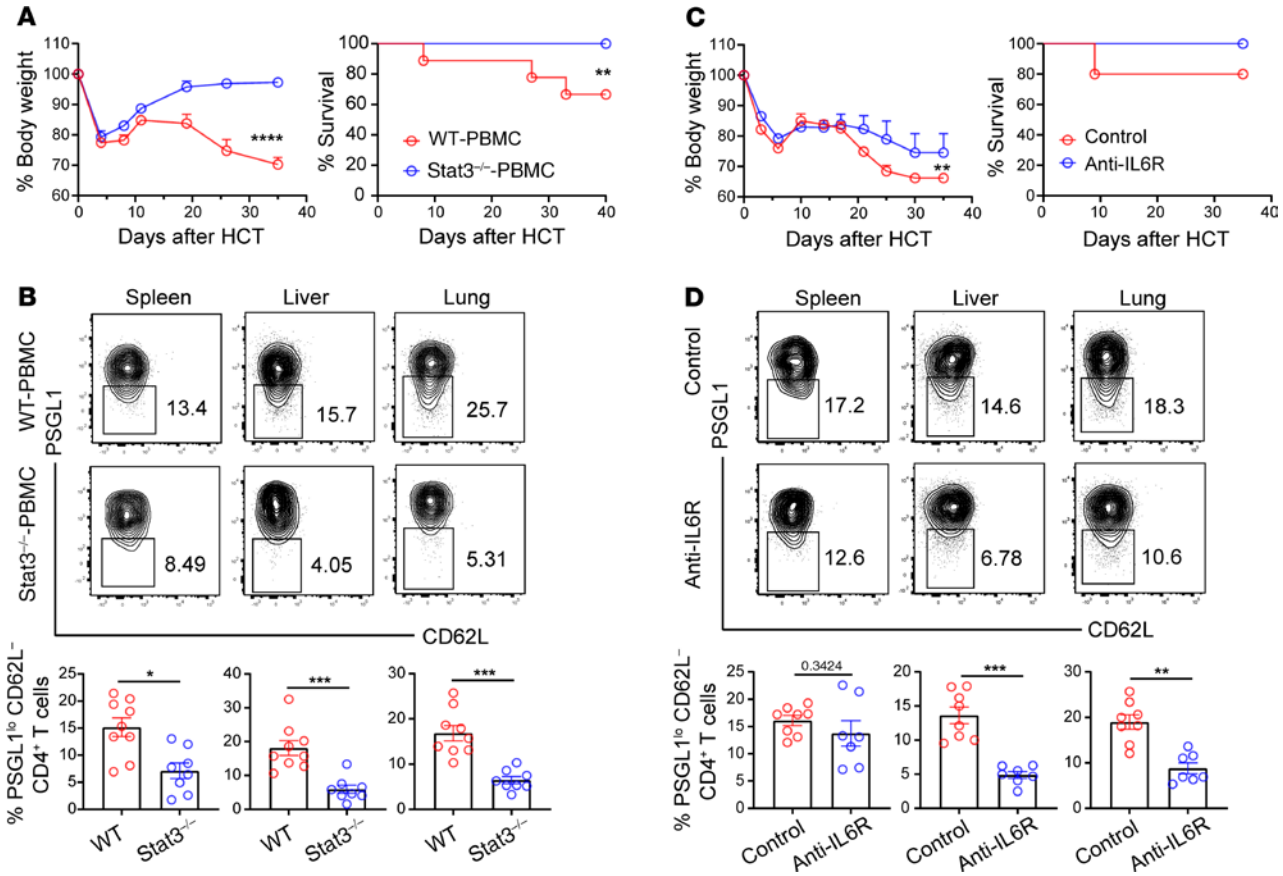

Figure 7. PSGL1^{hi}CD4^{+} T cells differentiate into PSGL1^{lo}CD4^{+} T cells in an IL6R-Stat3–dependent manner. BALB/c recipients were given 0.5M PBMCs from WT or Stat3$^{-/-}$ donors plus 2.5M TCD-BM from CD45.1 donors, and tissues were harvested at day 40 after HCT. (**A**) Curves of the survival percentage and percentage of body weight change. (**B**) Mononuclear cells from the spleen, liver, and lung were stained with anti–H-2Kb, CD45.1, TCRβ, CD4, CD62L, and PSGL1. Mean ± SEM of the percentage of donor-type H-2Kb^{+}PSGL1^{lo}CD62L^{-}CD4^{+}CD45.1^{-}TCRβ^{+} among donor-type CD4^{+} T cells is shown. *N* = 8–10, combined from at least 2 replicate experiments. (**C**) Recipients were treated with anti–IL-6R mAbs or control IgG weekly, and tissues were harvested 40 days after HCT. Curves of the survival percentage and percentage of body weight change. (**D**) Percentages of donor type of H-2Kb^{+}PSGL1^{lo}CD62L^{-}CD4^{+}CD45.1^{-}TCRβ^{+} cells among donor-type CD4^{+} T cells are shown. *N* = 6–8, combined from 2 replicate experiments. *P* values were calculated by correlation test or log-rank test (**A** and **C**) or unpaired 2-tailed Student's *t* tests (**B** and **D**). $^{*}P < 0.05$; $^{**}P < 0.01$; $^{***}P < 0.001$.

identified more than a decade ago by Craft et al. (9). We recently showed that PSGL1^{lo}CD4^{+} T cells are expanded in GVHD target tissues of autoimmune-like cGVHD mouse recipients that had destruction of lymphoid follicles (20). However, PSGL1^{lo}CD4^{+} T cells in humans have not been reported, and the function of PSGL-1^{lo}CD4^{+} T cells in nonlymphoid tissues remained unclear. Using a murine model of cGVHD that emerges from aGVHD (16) together with a humanized MHC$^{-/-}$HLA-A2^{+}DR4^{+} cGVHD model, we have demonstrated that both mouse and human PSGL1^{lo}CD4^{+} T cells in GVHD target tissues are PD1^{hi} tissue-resident B cell helpers that augment memory B cell differentiation into antibody-producing plasma cells through their PD1 interaction with PD-L2 on B cells. The extrafollicular PD1^{hi} PSGL1^{lo} B cell helpers from GVHD target tissues preferentially augment autoantibody production.

PD1^{hi}PSGL1^{lo}CD4^{+} T cells from GVHD target tissues are pathogenic tissue-resident B cell helpers. High PD1 expression can indicate anergy or exhaustion, as is the case for PD1^{+} Eomes^{+} T cells in target tissues of aGVHD (32), and PD1 deficiency in donor T cells exacerbates aGVHD (27). Other results, however, have shown that alloreactive T cells with upregulated expression of PD1 alone in GVHD patients are not anergic/exhausted (26). Consistently, both murine and human PD1^{hi}PSGL1^{lo}CD4^{+} T cells from GVHD target tissues downregulated expression of anergy markers TIM 3 and LAG3, upregulated expression of B cell helper markers of ICOS and IL-21, and upregulated expression of tissue-resident receptors CD69, CXCR6, and P2RX7. Our adoptive transfer and ex vivo coculture experiments showed that sorted murine and human PSGL1^{lo}CD4^{+} T cells from GVHD target tissues augmented memory B cell differentiation into antibody-producing plasma cells in a manner that depended on PD1 interaction with PD-L2. Taken collectively, we have demonstrated that murine and human PSGL1^{lo}CD4^{+} T cells are tissue-resident B cell helpers that do not circulate in the blood. They differ from PD1^{hi}CXCR5^{-} B cell helpers identified in human rheumatoid arthritis synovial fluid, a population that can circulate in the blood (33). They also differ from extrafollicular CXCR5^{-}CXCR4^{+}PSGL1^{lo}CD4^{+} T cells in the spleen of SLE mice (9) because they lack expression of CXCR4. The transcriptional regulation of PD1^{hi}PSGL1^{lo}CD4^{+} Trm cell differentiation has not been fully defined. CD8^{+} Trm cell differentiation in mice infected by herpes simplex virus is synergistically controlled by Hobit and Blimp 1 (34). Similarly, CD4^{+} Trm cell

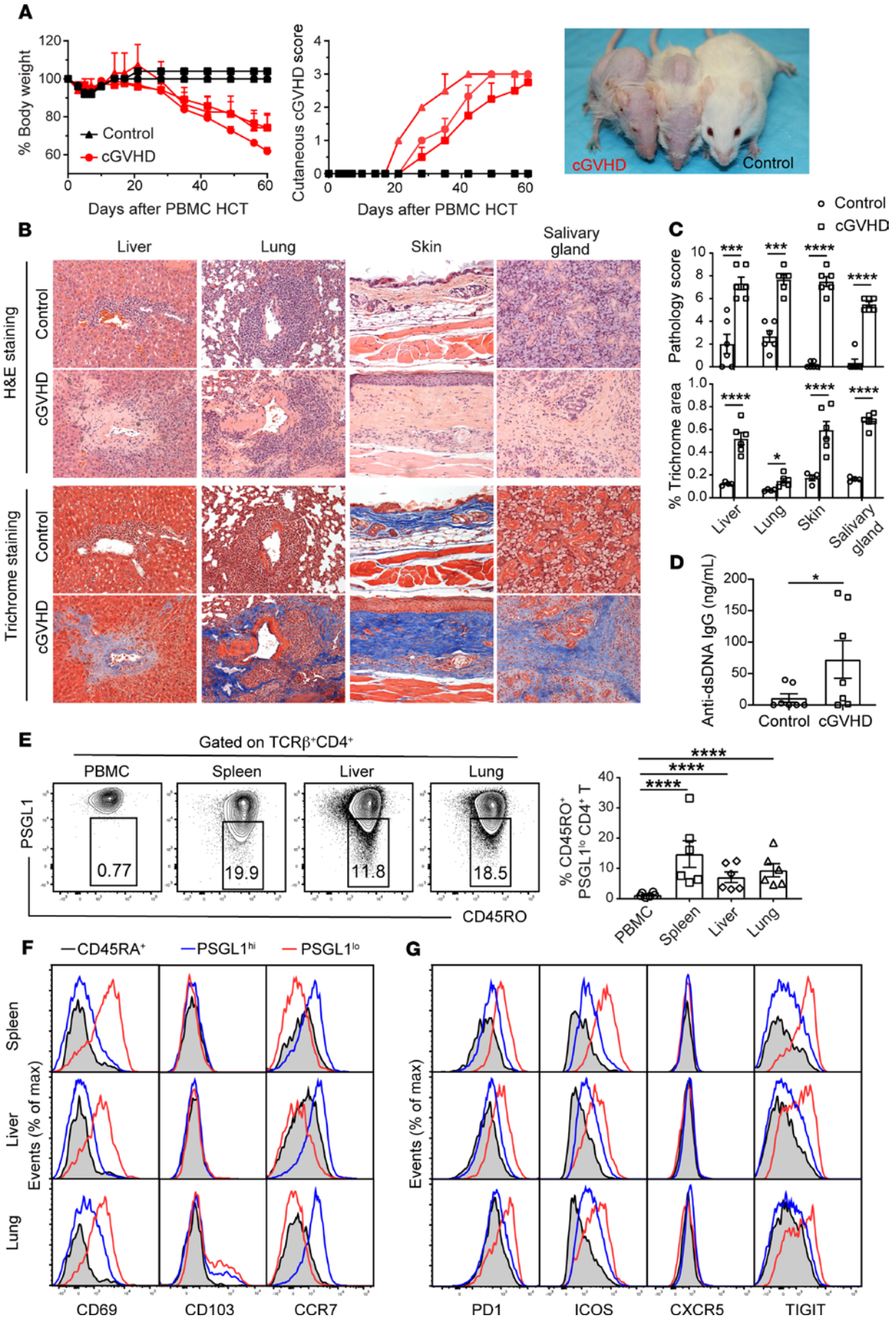

J Clin Invest. 2021;131(1):e135468 https://doi.org/10.1172/JCI135468

Figure 8. Human PBMCs give rise to tissue-resident PSGL1^{lo}CD4$^+$ T cells in humanized cGVHD mice. MHC$^{-/-}$ NSG or MHC$^{-/-}$HLA-A2$^+$DR4$^+$ NSG mice were treated with 200 cGy TBI followed by injection of freshly isolated PBMCs from 3 HLA-A2$^-$DR4$^-$ donors. PBMC from 3 donors were injected into 3 mice each. Recipients were monitored for development of GVHD for up to 60 days after HCT (**A**) Curves of percentage of body weight change and cutaneous GVHD score and representative photographs of 1 GVHD-free MHC$^{-/-}$ mouse and 2 GVHD MHC$^{-/-}$HLA-A2$^+$DR4$^+$ mice given the same human PBMCs. (**B**) Representative H&E and trichrome stains of liver, lung, skin, and salivary gland (original magnification, ×200). (**C**) Mean ± SEM of pathology score and trichrome staining areas. (**D**) Serum anti–dsDNA IgG concentration. (**E**) Representative flow cytometry patterns and mean ± SEM of percentage of PSGL1^{lo}CD4$^+$ T cells. (**F** and **G**) Surface marker expression of CD69, CCR7, CD103, PD1, ICOS, CXCR5, and TIGIT by PSGL1^{lo} in comparison with PSGL1^{hi} T cells from the spleen, liver, and lung of GVHD HLA-A2$^+$DR4$^+$ NSG recipients. One representative of 3 replicate experiments is shown. *P* values were calculated by 1-way ANOVA (**C**, **E**) or unpaired 2-tailed Student's *t* tests (**D**). $^*P < 0.05$; $^{**}P < 0.01$; $^{***}P < 0.001$.

differentiation and production of proinflammatory cytokines and chemokines is synergistically regulated by Hobit and Blimp1 (35). CD8$^+$ Trm cells shape local and systemic secondary T cell responses, and Hobit$^+$CD8$^+$ Trm cells can give rise to circulating memory T cells that do not express Hobit (36). In RNA-Seq analysis, we found that neither PSGL1^{lo} nor PSGL1^{hi} CD4$^+$ T cells from GVHD target tissues expressed detectable levels of Hobit, but they both expressed Blimp1, with no significant difference between them. Therefore, the transcriptional regulation of Trm cells in GVHD target tissues may differ from those in viral infection or autoimmune colitis (35). The role of Hobit, Blimp1, and other transcriptional factors in regulating CD4$^+$ Trm formation in GVHD target tissues is under investigation.

IgG autoantibodies produced by memory B cells that interact with PSGL1^{lo}CD4$^+$ T cells may augment fibrosis in GVHD target tissues. We observed that the presence of human PD1^{hi} PSGL-1^{lo}CD4$^+$ T cells, memory B cells, and IgG antibody deposition in the humanized NSG mice were associated with markedly enhanced fibrosis in the GVHD target tissues. This is consistent with reports that anti-PDGFR and anti–cell membrane antigen autoantibodies augment cGVHD in patients (37, 38). Other factors may also contribute to the fibrosis, because PSGL1^{lo}CD4$^+$ T cells produce IL-17 in addition to IL-21, IL-13, and IFN-γ (20). PD1$^+$IL-17–producing CD4$^+$ T cells mediated fibrosis in the lung (39).

Alloreactive CD4$^+$ T cell–derived autoreactive PSGL1^{lo}CD4$^+$ T cell interaction with B cells in GVHD target tissues augmented expansion of autoreactive B cells, leading to increased autoantibody production. HLA-A2$^{-/-}$DR4$^{-/-}$ human PBMCs showed little expansion of B cells or little increase of serum anti–dsDNA human IgG in MHC$^{-/-}$ NSG recipients, but they showed expansion of memory B and plasma cells and high-level serum anti–dsDNA human IgG in MHC$^{-/-}$A2$^+$DR4$^+$ NSG recipients, indicating that alloreactive CD4$^+$ T cells from human PBMCs can become autoreactive CD4$^+$ T cells in GVHD recipients and activate autologous autoreactive B cells to produce autoantibodies. This is consistent with our previous report in mouse models that alloreactive CD4$^+$ T cells become autoreactive T cells in cGVHD recipients (12). In addition, we found that the autoantibody production in cGVHD recipients was dependent on PSGL1^{lo}CD4$^+$ T cell PD1 interaction with PD-L2 on B cells in mouse models. This may result from PD-L2^{hi} B cells in different tissues presenting different antigens to expand different autoreactive PD1^{hi}PSGL-1^{lo}CD4$^+$ T cell clones. Our previous studies showed that CD4$^+$ T cell and B cell interactions led to clonal expansion of autoreactive CD4$^+$ T cells in cGVHD recipients (3).

Extrafollicular PSGL1^{lo}CD4$^+$ T cell interaction with B cells differs from PD1^{hi}Tfh interaction with B cells in the GC. PD1^{hi}Tfh interaction with GC B cells via PD1/PD-L2 was proposed to mediate negative selection of autoreactive CD4$^+$ Tfh cells, in addition to regulating GC B cell affinity maturation and formation of long-lived plasma cells (6, 40). The presence of extrafollicular autoreactive PD1^{hi}CD4$^+$ T cells, including PD1^{hi}CXCR5$^-$ Tfh-like cells in rheumatoid arthritis synovial tissues (33) and PD1^{hi}CXCR5$^-$PSGL1^{lo}CD4$^+$ T cells in the target tissues of cGVHD described in the current studies, may indicate a lack of negative selection against autoreactive PD1^{hi}CD4$^+$ T cells during T cell–B cell interaction in the inflammatory nonlymphoid tissues.

Autoreactive PD1^{hi}PSGL1^{lo}CD4$^+$ T cells may be derived from anergic/exhausted autoreactive T cells among PSGL1^{hi}CD4$^+$ T cells in the donor PBMCs. Autoreactive T cells are present in the periphery of healthy individuals, often with anergic or exhausted phenotype (41), but they can be revived by lymphopenia or by exposure to inflammation (42–44). Consistently, we observed that although all CD4$^+$ T cells in murine or human PBMCs were PSGL1^{hi} before HCT, both gave rise to PD1^{hi}PSGL1^{lo}CD4$^+$ T cells in GVHD target tissues of recipient mice. Development of PD1^{hi} PSGL1^{lo}CD4$^+$ T cells in mice depends on IL-6R/Stat3 signaling. Our observations could explain why infusion of granulocyte-colony stimulating factor (G-CSF)–mobilized blood grafts containing more donor T cells caused more severe autoimmune-like cGVHD, even though the severity of aGVHD was reduced (45, 46). Higher numbers of T cells in the graft may lead to more abundant autoreactive PD1^{hi}PSGL1^{lo}CD4$^+$ T cells that can augment the autoantibody production that worsens tissue damage.

PD1^{hi}PSGL1^{lo}CD4$^+$ T cell interaction with B cells indirectly augmented cutaneous cGVHD pathogenesis by augmenting antibody production outside skin tissues. We reported that donor B cells contribute to cGVHD pathogenesis through their antigen-presenting cell (APC) function that expanded pathogenic CD4$^+$ T cells as well as their production of antibodies. IgG antibodies from donor B cells were not required to initiate cGVHD, but were required for the persistence of cutaneous GVHD (3, 4). In the current studies, we found that donor-type B cells and PD1^{hi}PSGL1^{lo}CD4$^+$ B cell helpers were nearly undetectable in the skin tissue of cGVHD mice and humanized cGVHD mice, although both PD1^{hi}PSGL1^{lo}CD4$^+$ T cells and B cells were present in the liver and lung. We observed IgG deposition and fibrosis in the GVHD target tissues of humanized mice with expansion of donor-type B cells in the liver and lung, but not in control mice without expansion of donor-type B cells. Therefore, we propose that cutaneous fibrosis results from deposition of autoantibodies produced by B-lineage cells located in other tissues such as the liver and lung.

We believe that targeting tissue-resident T cells may represent a potentially novel approach for preventing and treating autoimmune-like cGVHD and other autoimmune diseases.

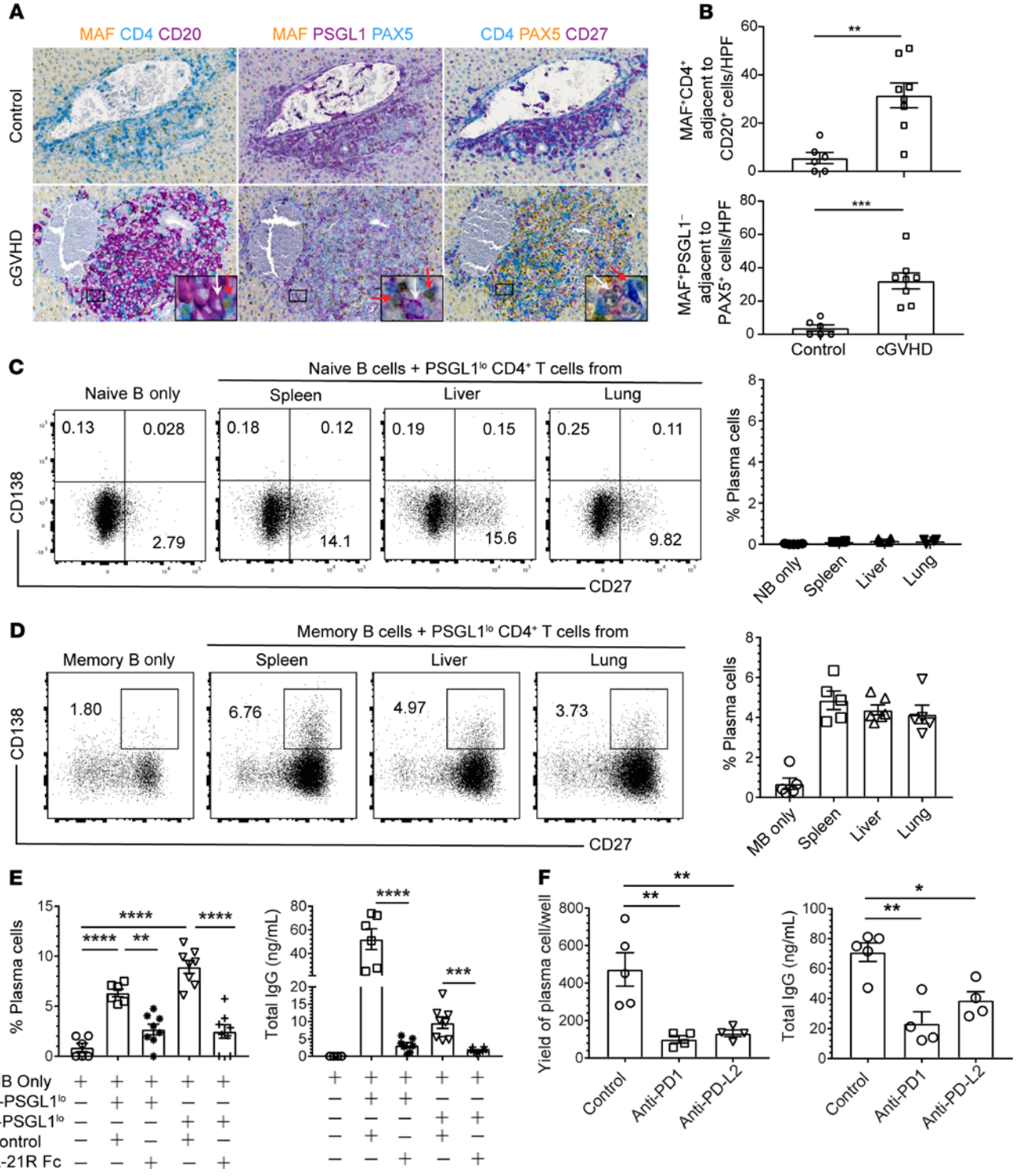

Figure 9. Human PBMC-derived tissue-resident PSGL1^{lo}CD4^{+} T cells augment autologous memory B cell differentiation into plasma cells with IgG antibody production. Humanized cGVHD mice were established as in Figure 8. (**A**) Adjacent 3 sections of liver tissues of control and cGVHD mice were stained with 1) anti–human MAF, CD4, and CD20; 2) anti–human MAF, PSGL1, and PAX5; or 3) anti–human CD4, PAX5, and CD27. White arrows point to B cells and red arrows point to T cells in different panels (original magnification, ×200; insets, ×800). (**B**) Quantification of total MAF^{+}CD4^{+} T cells and MAF^{+}PSGL1^{-} T cells adjacent to B cells in the liver tissues. (**C**–**F**) Human PSGL1^{lo}CD45RO^{+}CD4^{+} T cells from the spleen, liver, and lung of humanized cGVHD HLA-A2^{+}DR4^{+} NSG recipients 60 days after cell transfer were sorted and cocultured with sorted autologous naive or memory B cells from cryopreserved PBMC. (**C**) Naive B cells (NB) alone or cocultured with PSGL1^{lo}CD4^{+} T cells from the spleen, liver, or lung. Representative flow cytometry staining patterns of CD27 versus CD138 on B cells and percentages of plasma cells are shown. (**D**) Memory B cells (MB) alone or cocultured with PSGL1^{lo}CD4^{+} T cells from the spleen, liver, or lung. Representative flow cytometry patterns and percentages of plasma cells are shown. (**E**) Memory B cells cocultured with PSGL1^{lo}CD4^{+} T cells with or without neutralization of IL-21 with IL-21R-Fc. Percentages of plasma cells and IgG concentrations in culture supernatants are shown. (**F**) Memory B cells cocultured with PSGL1^{lo}CD4^{+} T cells with or without blocking anti-PD1 or anti–PD-L2. Yields of plasma cells and total IgG levels are shown. Each experiment was repeated at least twice. *P* values were calculated by unpaired 2-tailed Student's *t* tests (**B**) or 1-way ANOVA multiple-comparisons test (**E** and **F**). $^{*}P < 0.05$; $^{**}P < 0.01$; $^{***}P < 0.001$; $^{****}P < 0.0001$.

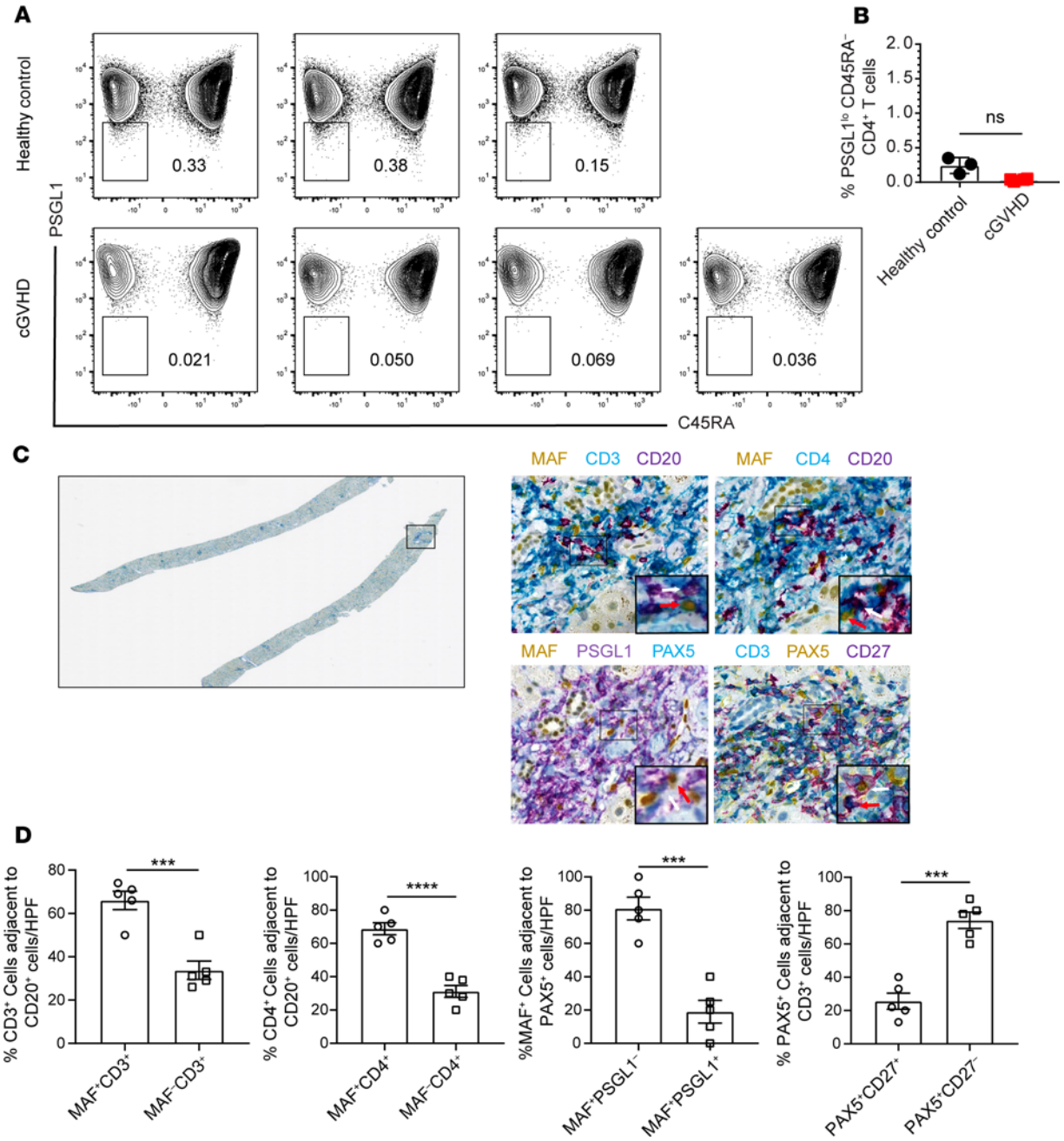

Figure 10. PSGL1^{lo} MAF^{+} CD4^{+} T cells and CD27^{+} memory B cells accumulate in the liver lesions of cGVHD patients. (**A**) PBMCs from healthy controls and cGVHD patients were stained with anti–human CD3, anti–human CD4, anti–human CD45RA, and anti–human PSGL1. Flow cytometry staining patterns of 3 healthy controls and 4 cGVHD patients, and (**B**) the mean ± SEM of percentage of PSGL1^{lo}CD45RA^{-}CD4^{+} T cells are shown. (**C**) IHC staining of 4 adjacent slides of liver biopsy tissues from cGVHD patient with (a) anti–human MAF, CD3, and CD20; (b) anti–human MAF, CD4, and CD20; (c) anti–human Maf, PSGL1, and PAX5; or (d) anti–human CD3, PAX5, and CD27. Representative result of 1 patient is shown for 5 cGVHD patients. White arrows point to B cells, and red arrows point to T cells (original magnification, ×400; insets, ×800). (**D**) Calculation of percentage of MAF^{+} T subsets or PAX5^{+} B cell subset that were juxtaposed to each other. *P* value was calculated by unpaired 2-tailed Student's *t* tests (**B** and **D**). $^{*}P < 0.05$; $^{**}P < 0.01$; $^{***}P < 0.001$; $^{****}P < 0.0001$.

In preclinical models, therapy with depleting anti-CD20 prevented autoimmune cGVHD and other autoimmune diseases, but did not effectively treat ongoing cGVHD or autoimmune diseases, because expression of CD20 was lost by activated B cells in the tissue (47, 48). Blockade of B cell receptor (BCR) signaling by the Bruton's Tyrosine Kinase (BTK) inhibitor Ibrutinib is effective in some patients with cGVHD and other autoimmune diseases (49, 50). Therefore, targeting B cells alone does not control autoimmune diseases or chronic GVHD in all cases. Administration of NAD that targets P2RX7 and augments apoptosis of Trm cells ameliorated colitis (35). It would be of interest to test whether targeting PSGL1^{lo}CD4^{+} Trm cells by NAD is effective for autoimmune diseases that do not improve after treatment with B cell–specific agents.

In summary, the current studies have unraveled new insights into T cell–B cell interactions in the nonlymphoid target tissues of

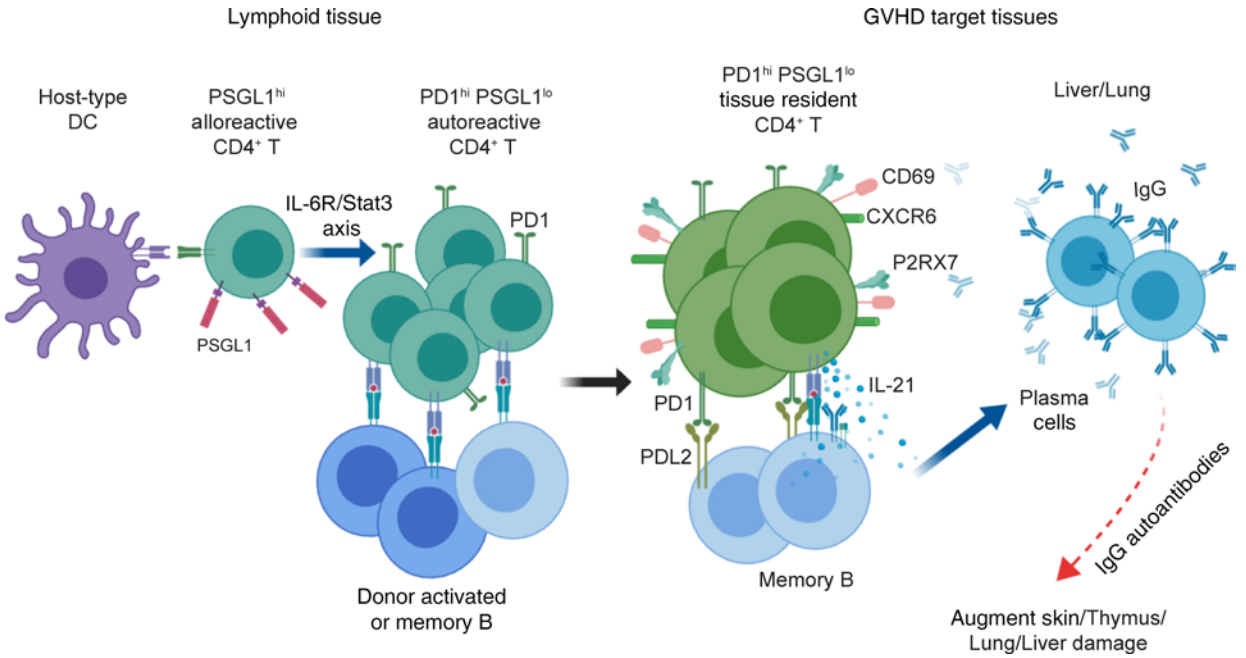

Figure 11. Development of tissue-resident PSGL1^{lo}CD4^{+} T cells and their interaction with B cells in GVHD target tissues. At acute GVHD phase, donor PSGL-1^{hi}CD4^{+} T cells interact with host APCs in the lymphoid tissues and differentiate into B cell helper of PD1^{hi}PSGL1^{lo}CD4^{+} T cells in a IL-6/Stat3-dependent manner. The PSGL1^{lo}CD4^{+} T cells infiltrate GVHD target tissues and differentiate into Trm cells by upregulating expression of CD69, CXCR6 and P2RX7. The PD1^{hi}CD4^{+} Trm cells augment memory B cell differentiation into plasma cells via their PD1 interaction with PD-L2 on the memory B cells and via secretion of IL-21. Plasma cells produce IgG antibodies that enter circulation and deposit in the GVHD target tissues such as skin to augment tissue damage during chronic GVHD phase.

cGVHD recipients. We propose that, as depicted in the diagram (Figure 11), donor-type alloreactive PSGL1^{hi}CD4^{+} T cells from the donor graft interact with host-type APCs in the lymphoid tissues and become activated PD1^{hi}PSGL1^{lo}CD4^{+} autoreactive T cells that recognize autoantigens presented by donor B cells. This interaction leads to activation of autoreactive B cells and production of IgG antibodies that augment damage in lymphoid tissues, resulting in lymphopenia, as described in our previous publication (20). In the GVHD target tissues, the PD1^{hi}PSGL1^{lo}CD4^{+} T cells differentiate into tissue-resident T cells with high expression of CD69, CXCR6, and P2RX7 in an IL-6R/Stat3–dependent manner. These cells may attract donor-type activated/memory B cells into the target tissues. At the same time, those PD1^{hi}PSGL1^{lo}CD4^{+} autoreactive T cells recognize autoantigens presented by the donor B cells and interact with the B cells via the TCR-MHC complex and other costimulatory molecules including PD1 and PD-L2. The interactions of T cell PD1 with B cell PD-L2 lead to enhanced production of IgG autoantibodies that augment tissue damage. Our study found that circulating IgG autoantibodies also deposited in the skin, thereby augmenting skin GVHD, although neither PSGL1^{lo}CD4^{+} T nor B cells infiltrated the skin. Our data indicated that PSGL1^{hi}CD4^{+} T cells can contribute to autoantibody-mediated cGVHD pathogenesis only by becoming PSGL1^{lo}CD4^{+} cells that acquire B cell helper function. The extent to which PSGL-1^{hi}CD4^{+} T cells contribute to the pathogenesis of cGVHD through autoantibody-independent mechanisms remains to be determined.

Methods

Mice. BALB/c and C57BL/6 mice were purchased from National Cancer Institute Laboratories. PD1$^{-/-}$ and PD-L1$^{-/-}$ C57BL/6 breeders were provided by Haidong Dong (Mayo Clinic, Rochester, Minnesota, USA) with the approval of Tasuku Honjo (Tokyo University, Tokyo, Japan). Spleen and bone marrow from PD-L2$^{-/-}$ C57BL/6 mice were provided by Karen M. Haas (Wake Forest School of Medicine, Winston-Salem, North Carolina, USA). MHC$^{-/-}$ NSG and MHC$^{-/-}$HLA-A2^{+}DR4^{+} mice were established by backcrossing β2m$^{-/-}$ MHC-II$^{-/-}$ NSG mice with HLA-A2^{+} or DR4^{+} NSG mice (The Jackson Laboratory) at the Animal Resources Center (ARC) of City of Hope.

GVHD patients and healthy donor information. The patients' information including gender, age, disease, graft type, conditioning, GVHD prophylaxis, and GVHD grade are detailed in Supplemental Table 1. Control subjects are detailed in Supplemental Table 2.

Experimental procedures. Experimental procedures including (a) induction and assessment of GVHD; (b) isolation of lymphocytes from GVHD target tissues; (c) antibodies, flow cytometry analysis, and cell sorting; (d) histopathology, IHC, and tissue immunofluorescent staining; (e) tissue IgG deposition; (f) RNA sequencing analysis; (g) ELISA of total IgG and anti–dsDNA IgG; (h) adoptive cell transfer; and (i) T cell–B cell cocultures have been described in previous publications (3, 4, 12, 16, 20, 33) and are described in Supplemental Methods.

Data availability. The RNA sequencing data have been deposited in the NCBI's Gene Expression Omnibus database (GEO, GSE157566).

Statistics. Data were shown as mean ± SEM. Comparison of percentage of survival in groups was analyzed by log-rank test. Two-group means comparison was analyzed by using an unpaired 2-tailed Student's *t* test. For evaluation of 3 means, we used 1-way ANOVA multiple-comparisons test (GraphPad Prism version 7). *P* values less than 0.05 were considered to be statistically significant.

Study approval. The City of Hope IRB approved the study, and all subjects provided written informed consent according to the protocols in IRB file 15172.

Author contributions

XK designed and perform experiments, acquired and analyzed data, and prepared the manuscript. XW and HQ performed RNA-sequencing and data analysis. Deye Zeng designed and performed experiments and acquired data. MS and BW performed immunofluorescent staining. SY, QS, YZ, MS, and UN assisted in experiments. KMH provided PD-L2$^{-/-}$ C57BL/6 mice and critical review of the manuscript. ADR provided advice for RNA-sequencing analysis, reviewed the manuscript, and provided financial support for this project. RN provided advice on human-related studies, organized human samples, and reviewed the manuscript. PJM provided advice on experimental design and critical review and editing of the manuscript. AH is Deye Zeng's PhD advisor. Defu Zeng designed and supervised the research and wrote the manuscript.

This work was supported by NIH grant R01 AI066008 and R01 CA228465 (to Defu Zeng), as well as supported by the Legacy Heritage Fund and National Cancer Institute grant P30CA033572.

Address correspondence to: Defu Zeng, The Beckman Research Institute of City of Hope; 1500 East Duarte Road, Duarte, California 91010, USA. Phone: 627.218.3587; Email dzeng@coh.org. Or to: Aimin Huang, Fujian Medical University, 1 Xueyuan Road, Minhou, Fuzhou, 350122, China. Phone: 86.0591.22862869; Email: aimin@fjmu.edu.cn.

1. Seth A, Craft J. Spatial and functional heterogeneity of follicular helper T cells in autoimmunity. *Curr Opin Immunol*. 2019;61:1–9.
2. Zhang C, et al. Donor CD4$^+$ T and B cells in transplants induce chronic graft-versus-host disease with autoimmune manifestations. *Blood*. 2006;107(7):2993–3001.
3. Young JS, et al. Donor B cells in transplants augment clonal expansion and survival of pathogenic CD4$^+$ T cells that mediate autoimmune-like chronic graft-versus-host disease. *J Immunol*. 2012;189(1):222–233.
4. Jin H, et al. Antibodies from donor B cells perpetuate cutaneous chronic graft-versus-host disease in mice. *Blood*. 2016;127(18):2249–2260.
5. Crotty S. T follicular helper cell biology: a decade of discovery and diseases. *Immunity*. 2019;50(5):1132–1148.
6. Good-Jacobson KL, Szumilas CG, Chen L, Sharpe AH, Tomayko MM, Shlomchik MJ. PD-1 regulates germinal center B cell survival and the formation and affinity of long-lived plasma cells. *Nat Immunol*. 2010;11(6):535–542.
7. Freeman GJ, et al. Engagement of the PD-1 immunoinhibitory receptor by a novel B7 family member leads to negative regulation of lymphocyte activation. *J Exp Med*. 2000;192(7):1027–1034.
8. Somers WS, Tang J, Shaw GD, Camphausen RT. Insights into the molecular basis of leukocyte tethering and rolling revealed by structures of P- and E-selectin bound to SLe(X) and PSGL-1. *Cell*. 2000;103(3):467–479.
9. Odegard JM, et al. ICOS-dependent extrafollicular helper T cells elicit IgG production via IL-21 in systemic autoimmunity. *J Exp Med*. 2008;205(12):2873–2886.
10. Ferrara JL, Levine JE, Reddy P, Holler E. Graft-versus-host disease. *Lancet*. 2009;373(9674):1550–1561.
11. Zeiser R, Blazar BR. Pathophysiology of chronic graft-versus-host disease and therapeutic targets. *N Engl J Med*. 2017;377(26):2565–2579.
12. Zhao D, et al. Alloimmune response results in expansion of autoreactive donor CD4$^+$ T cells in transplants that can mediate chronic graft-versus-host disease. *J Immunol*. 2011;186(2):856–868.
13. Tivol E, Komorowski R, Drobyski WR. Emergent autoimmunity in graft-versus-host disease. *Blood*. 2005;105(12):4885–4891.
14. Bleakley M, et al. Outcomes of acute leukemia patients transplanted with naive T cell-depleted stem cell grafts. *J Clin Invest*. 2015;125(7):2677–2689.
15. Zhang Y, Hexner E, Frank D, Emerson SG. CD4+ T cells generated de novo from donor hemopoietic stem cells mediate the evolution from acute to chronic graft-versus-host disease. *J Immunol*. 2007;179(5):3305–3314.
16. Wu T, et al. Thymic damage, impaired negative selection, and development of chronic graft-versus-host disease caused by donor CD4+ and CD8$^+$ T cells. *J Immunol*. 2013;191(1):488–499.
17. Sarantopoulos S, Ritz J. Aberrant B-cell homeostasis in chronic GVHD. *Blood*. 2015;125(11):1703–1707.
18. Radojcic V, et al. STAT3 signaling in CD4$^+$ T cells is critical for the pathogenesis of chronic sclerodermatous graft-versus-host disease in a murine model. *J Immunol*. 2010;184(2):764–774.
19. Flynn R, et al. Increased T follicular helper cells and germinal center B cells are required for cGVHD and bronchiolitis obliterans. *Blood*. 2014;123(25):3988–3998.
20. Deng R, et al. Extrafollicular CD4$^+$ T-B interactions are sufficient for inducing autoimmune-like chronic graft-versus-host disease. *Nat Commun*. 2017;8(1):978.
21. Masopust D, Soerens AG. Tissue-resident T cells and other resident leukocytes. *Annu Rev Immunol*. 2019;37:521–546.
22. Mueller SN, Mackay LK. Tissue-resident memory T cells: local specialists in immune defence. *Nat Rev Immunol*. 2016;16(2):79–89.
23. Oh JE, et al. Migrant memory B cells secrete luminal antibody in the vagina. *Nature*. 2019;571(7763):122–126.
24. Schroeder MA, DiPersio JF. Mouse models of graft-versus-host disease: advances and limitations. *Dis Model Mech*. 2011;4(3):318–333.
25. Yi T, et al. Reciprocal differentiation and tissue-specific pathogenesis of Th1, Th2, and Th17 cells in graft-versus-host disease. *Blood*. 2009;114(14):3101–3112.
26. Simonetta F, et al. Dynamics of expression of programmed cell death protein-1 (PD-1) on T cells after allogeneic hematopoietic stem cell transplantation. *Front Immunol*. 2019;10:1034.
27. Blazar BR, et al. Blockade of programmed death-1 engagement accelerates graft-versus-host disease lethality by an IFN-γ-dependent mechanism. *J Immunol*. 2003;171(3):1272–1277.
28. Shapiro-Shelef M, Calame K. Regulation of plasma-cell development. *Nat Rev Immunol*. 2005;5(3):230–242.
29. Yu H, Pardoll D, Jove R. STATs in cancer inflammation and immunity: a leading role for STAT3. *Nat Rev Cancer*. 2009;9(11):798–809.
30. Chen X, et al. Blockade of interleukin-6 signaling augments regulatory T-cell reconstitution and attenuates the severity of graft-versus-host disease. *Blood*. 2009;114(4):891–900.
31. Kennedy GA, et al. Addition of interleukin-6 inhibition with tocilizumab to standard graft-versus-host disease prophylaxis after allogeneic stem-cell transplantation: a phase 1/2 trial. *Lancet Oncol*. 2014;15(13):1451–1459.
32. Ni X, et al. PD-L1 interacts with CD80 to regulate graft-versus-leukemia activity of donor CD8$^+$ T cells. *J Clin Invest*. 2017;127(5):1960–1977.
33. Rao DA, et al. Pathologically expanded peripheral T helper cell subset drives B cells in rheumatoid arthritis. *Nature*. 2017;542(7639):110–114.
34. Mackay LK, et al. Hobit and Blimp1 instruct a universal transcriptional program of tissue residency in lymphocytes. *Science*. 2016;352(6284):459–463.
35. Zundler S, et al. Hobit- and Blimp-1-driven CD4$^+$ tissue-resident memory T cells control chronic intestinal inflammation. *Nat Immunol*. 2019;20(3):288–300.
36. Behr FM, et al. Tissue-resident memory CD8$^+$ T cells shape local and systemic secondary T cell responses. *Nat Immunol*. 2020;21(9):1070–1081.
37. Wang KS, et al. Antibodies targeting surface membrane antigens in patients with chronic graft-versus-host disease. *Blood*. 2017;130(26):2889–2899.
38. Svegliati S, et al. Stimulatory autoantibodies to PDGF receptor in patients with extensive chronic graft-versus-host disease. *Blood*. 2007;110(1):237–241.
39. Celada LJ, et al. PD-1 up-regulation on CD4$^+$ T cells promotes pulmonary fibrosis through STAT3-mediated IL-17A and TGF-β1 production. *Sci Transl Med*. 2018;10(460):eaar8356.
40. Shi J, Hou S, Fang Q, Liu X, Liu X, Qi H. PD-1 controls follicular T helper cell positioning and function. *Immunity*. 2018;49(2):264–274.e4.
41. Wherry EJ, Kurachi M. Molecular and cellular insights into T cell exhaustion. *Nat Rev Immunol*. 2015;15(8):486–499.
42. King C, Ilic A, Koelsch K, Sarvetnick N. Homeostatic expansion of T cells during immune insufficiency generates autoimmunity. *Cell*. 2004;117(2):265–277.
43. Calzascia T, et al. CD4 T cells, lymphopenia, and IL-7 in a multistep pathway to autoimmunity.

Proc Natl Acad Sci U S A. 2008;105(8):2999–3004.
44. Bennett L, et al. Interferon and granulopoiesis signatures in systemic lupus erythematosus blood. *J Exp Med*. 2003;197(6):711–723.
45. MacDonald KP, et al. Chronic graft-versus-host disease after granulocyte colony-stimulating factor-mobilized allogeneic stem cell transplantation: the role of donor T-cell dose and differentiation. *Biol Blood Marrow Transplant*. 2004;10(6):373–385.
46. Levine JE, et al. Cytokine-mobilized allogeneic peripheral blood stem cell transplants in children result in rapid engraftment and a high incidence of chronic GVHD. *Bone Marrow Transplant*. 2000;25(1):13–18.
47. Johnston HF, et al. Administration of anti-CD20 mAb is highly effective in preventing but ineffective in treating chronic graft-versus-host disease while preserving strong graft-versus-leukemia effects. *Biol Blood Marrow Transplant*. 2014;20(8):1089–1103.
48. Serreze DV, et al. Loss of intra-islet CD20 expression may complicate efficacy of B-cell-directed type 1 diabetes therapies. *Diabetes*. 2011;60(11):2914–2921.
49. Ryan CE, et al. Ibrutinib efficacy and tolerability in patients with relapsed chronic lymphocytic leukemia following allogeneic HCT. *Blood*. 2016;128(25):2899–2908.
50. Waller EK, et al. Ibrutinib for chronic graft-versus-host disease after failure of prior therapy: 1-year update of a phase 1b/2 study. *Biol Blood Marrow Transplant*. 2019;25(10):2002–2007.